

Option Pricing with Time-Varying Volatility Risk Aversion*

Peter Reinhard Hansen^{a†} and Chen Tong^{b,c}

^a*University of North Carolina & Copenhagen Business School*

^b*Department of Finance, School of Economics, Xiamen University*

^c*Wang Yanan Institute for Studies in Economics, Xiamen University*

October 18, 2022

Abstract

We introduce a novel pricing kernel with time-varying *variance risk aversion* that yields closed-form expressions for the VIX. We also obtain closed-form expressions for option prices with a novel approximation method. The model can explain the observed time-variation in the shape of the pricing kernel.

We estimate the model with S&P 500 returns and option prices and find that time-variation in volatility risk aversion brings a substantial reduction in derivative pricing errors. The variance risk ratio emerges as a fundamental variable and we show that it is closely related to economic fundamentals and key measures of sentiment and uncertainty.

Keywords: Pricing Kernel, Volatility Risk Aversion, GARCH, Heston-Nandi, Option Pricing, Score-driven

JEL Classification: G12, G13, C51, C52

*We are grateful to Szabolcs Blazsek, Jens Jackwerth, Tobias Sichert, and conference participants at the SoFiE 2022 conference for valuable comments.

†Address: University of North Carolina, Department of Economics, 107 Gardner Hall Chapel Hill, NC 27599-3305

1 Introduction

The pricing kernel is a fundamental concept in economics with roots in Arrow-Debreu securities, see [Arrow and Debreu \(1954\)](#). The pricing kernel is the ratio of risk neutral state probabilities and physical state probabilities. The [Lucas \(1978\)](#) tree model is a cornerstone of asset pricing theory, and it implies a pricing kernel that is monotonically decreasing in aggregate wealth. The pricing kernel can be estimated from asset and derivative prices, see e.g. [Aït-Sahalia and Lo \(2000\)](#), [Jackwerth \(2000\)](#) and [Rosenberg and Engle \(2002\)](#), and this literature has uncovered a number of stylized facts that are known as pricing kernel puzzles. One puzzle is that the empirical pricing kernel is upward sloping in some regions when plotted against the market return. This is at odds with the Lucas tree model and many other models, including the Heston-Nandi GARCH (HNG) model that yields closed-form expressions for option prices in a model with time-varying volatility, see [Heston and Nandi \(2000\)](#).

[Christoffersen et al. \(2013\)](#) generalized the HNG model to accommodate non-monotonicity in the pricing kernel. This was achieved by adding a variance risk premium to the model in addition to the equity risk premium. The resulting model is tractable, yields close-form expressions for option prices, and is popular in this literature. The shape of the pricing kernel in [Christoffersen et al. \(2013\)](#) is defined by the variance risk premium. A negative variance risk premium induces a U -shaped pricing kernel, which is the shape they find in their empirical analysis.

Although the framework in [Christoffersen et al. \(2013\)](#) can resolve one pricing puzzle, it is at odds with another stylized fact, which is that the shape of the pricing kernel is time-varying. The pricing kernel is typically found to have an U -shape when estimated over long sample periods, see e.g. [Cuesdeanu and Jackwerth \(2018\)](#). But it has distinctly different shapes in some periods, such as the years leading up to the global financial crisis. The time variation in the pricing kernel can be expressed as time-variation in the probability weighting function. [Polkovnichenko and Zhao \(2013\)](#) estimate the probability weighting function non-parametrically and find evidence that it is time varying. When individuals overweight low-probability events and underweight events with high probabilities it will result in a probability weighting function with an inverse S -shaped (and a U -shaped pricing kernel). This is the shape that [Polkovnichenko and Zhao \(2013\)](#) obtain empirically during most of their sample period. But the estimated weighting function has a regular S -shaped during the years 2004–2007, which implies that tail events are underweighted. This is consistent with the negative risk aversion function documented in [Aït-Sahalia and Lo \(2000\)](#) and [Jackwerth \(2000\)](#). Similar results were obtained in [Chabi-Yo and Song \(2013\)](#) and the inverted shape is also implied by DAX 30 options during the same years, see [Grith et al. \(2017\)](#). Time-variation is also documented by [Kiesel and Rahe \(2017\)](#) and by [Beare and Schmidt \(2016\)](#). The latter developed a formal statistical test for monotonicity and used it to identify days with unusual shapes. Interestingly, figure 3 in [Christoffersen et al. \(2013\)](#)

also contains evidence of a pricing kernel whose shape varies over time. For most calendar years, the empirical pricing kernel is U -shaped, however in some calendar years it has an inverted U -shape.¹ The inverted U -shape can be induced by (unmodeled) parameter instability, such as structural breaks, see [Sichert \(2022\)](#), and Markov switching dynamics see [Tong et al. \(2022\)](#).

In this paper, we make six main contribution. First, we propose a novel framework for derivative pricing that is based on a pricing kernel with time-varying risk aversion. When this pricing kernel is combined with the GARCH model of [Heston and Nandi \(2000\)](#), the risk neutral conditional variance divided by the physical conditional variance, $\eta_t = h_t^*/h_t$, emerges as a fundamental quantity. We will refer to η_t as the *variance risk ratio*. The variance risk ratio is responsible for time-variation in the pricing kernel and η_t is functionally linked to the risk aversion parameters that define the curvature of the pricing kernel. We show that the proposed framework can generate pricing kernels with the variety of shapes that are seen empirically. Importantly, the framework can also explain the observed time-variation in the empirical pricing kernels.

Second, we proceed to derive closed-form expressions for the VIX and option prices when η_t is time-varying. There are important differences between the case where the future path for η_t is predetermined and the case where it is driven by a stochastic process. In the former case, the pricing kernel has an affine structure and close-form expressions are available from the moment-generating function for cumulative returns. The affine structure is lost when the future path for η_t is random, and it is not possible to derive closed-form expressions for option prices with conventional methods. However, for this situation we develop a novel method that builds on the results for the the predetermined case, and applies a Taylor expansion to approximate the MGF for the stochastic case. This analytical approximation method work remarkably well, which we demonstrate empirically and by simulation methods.

The third contribution is an empirical implementation of the theoretical framework. We achieve this by connecting the autoregressive model for η_t with observed data using an observation-driven model for η_t . This is a natural choice because time-variation in volatility is modeled with an observation-driven model. Specifically, we propose a score-driven model, see [Creal et al. \(2013\)](#), where the first-order conditions of the log-likelihood function define innovation in η_t . This approach is intuitive because η is revised in the direction that reduces the expected pricing errors. A key advantage of observation-driven models is that they are simple to estimate. This is particular useful in the present context where the model will be estimates with a long sample and a large panel of option prices.

The fourth contribution is an empirical application with 32 years of daily S&P 500 returns, the CBOE VIX, and a panel of option prices. The estimation incorporates infor-

¹The authors do not comment on this observation, but do estimate a more flexible structure, which is not based on a pricing kernel with a fixed shape. See [Christoffersen et al. \(2013, figure 6\)](#).

mation from both the physical probability measure and the risk-neutral probability measure, as advocated by [Chernov and Ghysels \(2000\)](#). The empirical results show that time variation in the pricing kernel typically reduce pricing errors by 50%, or more, as measured by the root mean square error. This reduction is achieved for both VIX prices and option prices, is found both in-sample and out-of-sample, and the reduction is robust across key characteristics of options, such as moneyness, time to maturity, and the contemporaneous VIX level. The estimated time variation in the shape of the pricing kernel is consistent with the earlier literature on this. The estimated model produce a pricing kernel with an inverted hump shape during the years 2004 to 2007, and an inverted shape is also seen during periods around 1993 and around 2017.

Fifth, we connect the variance risk ratio with key asset pricing variables. Since the variance risk ratio, η_t , emerges as a fundamental variable, it is interesting to investigate how it relates to other key variables in this literature. Several variables have been tied to pricing kernel puzzles. For instance, investors with heterogeneous beliefs and disagreements about the physical distribution can bring about a U -shaped pricing kernel. The U -shape arises as a consequence of aggregation of investors who take opposite position in the market due to different beliefs about expected returns. Time variation in the level of disagreement would translate to time-variation in the pricing kernel, see e.g. [Shefrin \(2001, 2008\)](#), [Bakshi and Madan \(2008\)](#), [Bakshi et al. \(2010\)](#). A similar argument can be made about sentiment and uncertainty among investors, see e.g. [Han \(2008\)](#), [Polkovnichenko and Zhao \(2013\)](#), [Baker et al. \(2016\)](#), and [Bollerslev et al. \(2018\)](#). [Bali and Zhou \(2016\)](#) argue that market uncertainty can be approximated by the variance risk premium (VRP), see [Carr and Wu \(2008\)](#). The variance risk ratio, η_t , is obviously related to the VRP, which has been shown to predicts stock returns, see [Bollerslev et al. \(2009\)](#). A straight forward explanation is that preferences are state-dependent, with market uncertainty as a possible state variable, see e.g. [Grith et al. \(2017\)](#). We connect our results with this literature by showing that the monthly average of the variance risk ratio, η_t , is closely related to commonly used measures of sentiment, uncertainty, disagreement, etc. as well as other economic variables that are commonly used in this literature.

Sixth, the proposed model offers robustness to model misspecification. In the present context, the inverted U -shape could be an artifact of model misspecification, including parameter instability. If the Heston-Nandi GARCH model does not properly capture the dynamic properties of physical volatility, then it could overpredicts the physical volatility to an extend that induces a fictitious inverted U -shape. In this scenario the parameter, η_t , serves to compensate for misspecification. The score-based updating continuously adapts the pricing formula to eliminate predictable pricing errors regardless of their origin. This includes pricing errors induced by model misspecification. We discuss the implication of this in greater details in Section [5.5](#).

Our paper is related to, and builds on, a large body of literature. This includes the

literature that sought to explain the pricing kernel puzzles by augmenting existing models with additional state variables, see e.g. [Chabi-Yo et al. \(2008\)](#), [Chabi-Yo \(2012\)](#), [Brown and Jackwerth \(2012\)](#) and [Song and Xiu \(2016\)](#). The variance risk ratio, η_t , can be interpreted as an additional state variable that emerges naturally from our model structure. Our paper is also related to [Barone-Adesi et al. \(2008\)](#), who estimate a GJR GARCH model for returns under the physical measure. They do not specify a pricing kernel, but simply assume that the model under the risk neutral measure is also a GJR GARCH model, whose time-varying parameters are calibrated to minimize pricing errors in daily options. We also seek to minimize pricing errors through the inclusion of a corresponding term in the log-likelihood function, but our approach is fundamentally different. Our starting point is a pricing kernel and a model for the physical probability measure, \mathbb{P} , which define the model under \mathbb{Q} . In their empirical comparison, [Christoffersen et al. \(2013\)](#) also explored the same ideas as in [Barone-Adesi et al. \(2008\)](#), and estimated separate HNG models under both \mathbb{P} and \mathbb{Q} . They referred to this structure as an *ad-hoc model*, because it is not deduced from their pricing kernel. We show that the pricing kernel with a time varying variance risk ratio is incoherent with HNG models (with constant parameters) under both \mathbb{P} and \mathbb{Q} . Another related literature is that on time-varying risk aversion, because it is connected with the local shape of the pricing kernel. A seminal paper with time-varying risk aversion is [Campbell and Cochrane \(1999\)](#). Building on their framework, [Li \(2007\)](#) showed how time-varying risk aversion interacts with time-varying risk premium. Moreover, [González et al. \(2018\)](#) find that time-varying risk aversion is one of the main determinants of stock market betas. A recent paper by [Bekaert et al. \(2020\)](#) introduced a no-arbitrage asset pricing model with a time-varying risk aversion, for the pricing of equities and corporate bonds where the risk aversion is driven by the uncertainty shock.

The rest of the paper is organized as follows. We present the theoretical model in Section 2 and derive closed-form pricing formulae for the VIX and option prices in Section 3. In Section 3 we introduce a score-driven model for the variance risk ratio. An empirical application with 32 years of S&P 500 returns, VIX, and option prices is presented in Section 5. We show that the variance risk ratio relates to well-known measures of sentiment, disagreement, and uncertainty in Section 6. A summary and some concluding remarks are presented in Section 7. All proofs are given in Appendix.

2 The Model

The observed variables include the daily returns, $R_t \equiv \log(S_t/S_{t-1})$, where S_t is the underlying asset price on day t , and a vector of derivative prices, denoted X_t . We will work with two filtrations, $\mathcal{F}_t = \sigma(\{R_j, X_j\}, j \leq t)$ and $\mathcal{G}_t = \sigma(\{R_j, X_{j-1}\}, j \leq t)$, where the latter arises naturally from a factorization of the likelihood function. We obviously have $\mathcal{G}_t \subset \mathcal{F}_t$ for all t . We model returns with the classical Heston-Nandi GARCH model, which has a

convenient structure for derivative pricing. This model is given by the two equations:

$$R_{t+1} = r + (\lambda - \frac{1}{2})h_{t+1} + \sqrt{h_{t+1}}z_{t+1}, \quad (1)$$

$$h_{t+1} = \omega + \beta h_t + \alpha(z_t - \gamma\sqrt{h_t})^2, \quad (2)$$

where r is the risk free rate; λ is the equity risk premium; and $h_{t+1} = \text{var}(R_{t+1}|\mathcal{F}_t)$ is the daily conditional variance, see [Heston and Nandi \(2000\)](#). The return shock, z_{t+1} , is assumed to be independent and identically distributed (iid) with a standard normal distribution, $N(0, 1)$. The HNG model captures time-variation in the conditional variance, as is the case for ARCH and GARCH models, see [Engle \(1982\)](#) and [Bollerslev \(1986\)](#). But the HNG model also allows for dependence between returns and volatility (leverage). It is simple to verify that $\text{cov}_{t-1}(R_t, h_{t+1}) = -2\gamma\alpha h_t$, which shows that the magnitude of the leverage effect is defined by γ . A leverage effect is required to generate the empirically important smile in option prices. The dynamic structure of the HNG model is carefully crafted to yield a closed-form solution for option valuation, and [Heston and Nandi \(2000\)](#) showed that the continuous limit of the HNG model (as the time interval between observations shrinks to zero) yields a variance process, h_t , that converges weakly to a continuous-time square-root variance process, see [Feller \(1951\)](#), [Cox et al. \(1985\)](#), and [Heston \(1993\)](#).

Option pricing with GARCH models is possible with a simple risk-neutralization by [Duan \(1995\)](#), known as the *locally risk-neutral valuation relationship* (LRNVR). This method is equivalent to a pricing kernel with a risk premium for equity risk, see [Huang et al. \(2017\)](#). Unfortunately, the LRNVR pricing kernel is inadequate for explaining many differences between \mathbb{P} and \mathbb{Q} , including the variance risk premium, see [Hao and Zhang \(2013\)](#) and [Christoffersen et al. \(2013\)](#). We review their model next and then proceed to introduce the time-varying variance risk premium.

2.1 Pricing Kernel with Constant Parameters (CHNG)

[Christoffersen et al. \(2013\)](#) generalized the HNG model and we refer to this model as the CHNG model. The pricing kernel introduced in [Christoffersen et al. \(2013\)](#) is given by:

$$\frac{M_{t+1}}{M_t} = \left(\frac{S_{t+1}}{S_t}\right)^\phi \exp[\delta + \pi h_{t+1} + \xi(h_{t+2} - h_{t+1})],$$

and [Corsi et al. \(2013\)](#) showed that it can conveniently be expressed as

$$M_{t+1,t} = \frac{M_{t+1}}{\mathbb{E}_t M_{t+1}} = \frac{\exp[\phi R_{t+1} + \xi h_{t+2}]}{\mathbb{E}_t[\exp(\phi R_{t+1} + \xi h_{t+2})]}, \quad (3)$$

where the conditional expectation is taken with respect to the natural filtration for returns under \mathbb{P} , i.e. $\mathbb{E}_t(\cdot) = \mathbb{E}^{\mathbb{P}}(\cdot|R_t, R_{t-1}, \dots)$. The expression above shows that the pricing kernel depends on both equity risk and variance risk, where the magnitude of variance risk is

characterized by the parameter ξ . The equity risk is govern by ϕ , as well as ξ , because h_{t+2} depends on R_{t+1} . This structure implies the following dynamic under the risk neutral measure,

$$\begin{aligned} R_{t+1} &= r - \frac{1}{2}h_{t+1}^* + \sqrt{h_{t+1}^*}z_{t+1}^* \\ h_{t+1}^* &= \omega^* + \beta^*h_t^* + \alpha^*(z_t^* - \gamma^*\sqrt{h_t^*})^2, \end{aligned}$$

with $z_{t+1}^* \sim iid N(0, 1)$ and following relationships between parameters under \mathbb{P} and \mathbb{Q}

$$h_t^* = h_t\eta, \quad \omega^* = \omega\eta, \quad \beta^* = \beta, \quad \alpha^* = \alpha\eta^2, \quad \gamma^* = \gamma - \phi, \quad \eta = (1 - 2\alpha\xi)^{-1}. \quad (4)$$

The logarithm of the pricing kernel is a quadratic function of the daily market return,

$$\log \frac{M_t}{M_{t-1}} = -\lambda(R_t - r) + \xi\alpha \frac{(R_t - r)^2}{h_t} + \kappa_0 + \kappa_1 h_t, \quad (5)$$

where $\kappa_0 = \delta + \xi\omega + \phi r$ and $\kappa_1 = \pi + \xi(\beta - 1 + \alpha(\lambda - \frac{1}{2} + \gamma)^2)$, see [Christoffersen et al. \(2013\)](#). This shows that λ and ξ define the linear and quadratic terms, respectively. The former, λ , is the equity risk premium, whereas ξ governs the variance risk premium and $\xi > 0$ is associated with a U -shaped relationship between $\log M_t/M_{t-1}$ and returns.

Empirically, this relationship tends to be U -shaped, but it is not stable over time as can be seen in [Christoffersen et al. \(2013, figure 3\)](#). Figure 1 includes parts of figures 3 and 5 in [Christoffersen et al. \(2013\)](#). The four left panels are based on model-free market prices and the corresponding four right panels are based on model prices using their estimated model. There are periods where the relationship has an inverted U-shape, such as the years 2004-2007 (of which 2005 and 2006 are shown in Figure 1), which is incompatible with a static quadratic coefficient is constant.

2.2 Dynamic Pricing Kernel by means of Variance Risk Aversion

We seek a more flexible pricing kernel that is coherent with the observed variation over time. Expression (5) motivates a structure where ξ is time-varying ξ , because ξ defines the quadratic term. Next, we introduce our model with time-varying ξ , while maintaining the Heston-Nandi GARCH structure under \mathbb{P} .

Assumption 1. *Returns are given by the Heston-Nandi GARCH model, (1)-(2), under \mathbb{P} .*

Assumption 2. *The pricing kernel takes the form:*

$$M_{t+1,t} = \frac{\exp(\phi_t R_{t+1} + \xi_t h_{t+2})}{\mathbb{E}_t^{\mathbb{P}}[\exp(\phi_t R_{t+1} + \xi_t h_{t+2})]},$$

where ϕ_t and ξ_t are \mathcal{G}_t -measurable, and $\mathbb{E}_t^{\mathbb{P}}(\cdot) \equiv \mathbb{E}^{\mathbb{P}}(\cdot | \mathcal{G}_t)$.

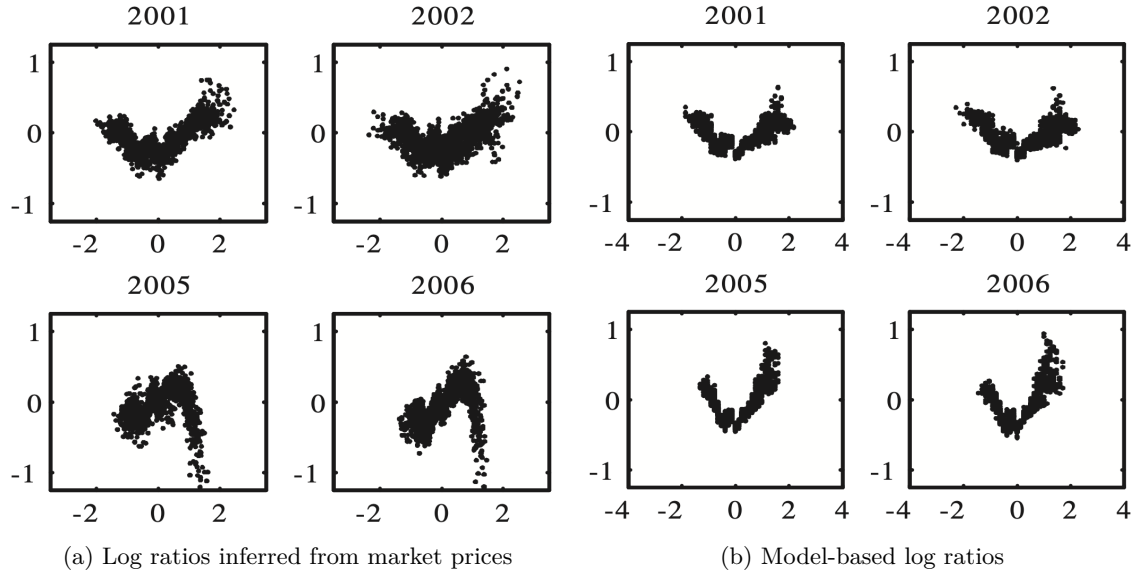


Figure 1: Log ratios of risk-neutral one-month densities and physical one-month histogram against log returns in monthly standard deviations. Panels (a) and (b) are subsets of figures 3 and 5, respectively, in [Christoffersen et al. \(2013\)](#). The former is based on empirical market prices and the latter has the corresponding model-based log ratios.

We can now present the dynamic properties under \mathbb{Q} .

Theorem 1. *Suppose Assumptions 1 and 2 hold and define $\eta_t \equiv (1 - 2\alpha\xi_t)^{-1}$.*

(i) *The two risk aversion parameters both depend on the variance risk ratio*

$$\xi_t = \frac{1}{2\alpha} \frac{\eta_t - 1}{\eta_t}, \quad \phi_t = \frac{\eta_t - 1}{\eta_t} \left(\gamma - \frac{1}{2} \right) - \frac{1}{\eta_t} \lambda,$$

(ii) *The return dynamics under risk neutral probability measure \mathbb{Q} is given by:*

$$\begin{aligned} R_{t+1} &= r - \frac{1}{2} h_{t+1}^* + \sqrt{h_{t+1}^*} z_{t+1}^*, \\ h_{t+1}^* &= \omega_t^* + \beta_t^* h_t^* + \alpha_t^* (z_t^* - \gamma_{t-1}^* \sqrt{h_t^*})^2, \end{aligned} \tag{6}$$

with $z_{t+1}^* \sim iid N(0, 1)$ and following relations between \mathbb{P} and \mathbb{Q} parameters:

$$\omega_t^* = \omega \eta_t, \quad \beta_t^* = \beta \frac{\eta_t}{\eta_{t-1}}, \quad \alpha_t^* = \alpha \eta_t \eta_{t-1}, \quad \gamma_t^* = \frac{1}{\eta_t} \left(\gamma + \lambda - \frac{1}{2} \right) + \frac{1}{2}$$

(iii) *We have*

$$\eta_t = \frac{h_{t+1}^*}{h_{t+1}}. \tag{7}$$

Theorem 1 reveals several interesting features of the risk neutral probability measure and its dynamic properties. First, the *variance risk ratio*, η_t , emerges as a fundamental

quantity.² This variable appears in all expressions that relate \mathbb{P} and \mathbb{Q} , and it has a straight forward interpretation. Its functional relationship with ξ_t , shows that η_t is an indirect measure of aversion to volatility risk. When η is large, agents require a large compensation for taking on variance risk, while a small value of η corresponds to a large appetite for variance risk. Note that ξ_t is positive if $\eta_t > 1$, which generates a U -shape in (5) whereas the inverted U -shape arises if $\eta_t < 1$, which implies $\xi_t < 0$.³

An important reason for allowing the variance risk ratio to be time-varying is that it permits h_t^* to depend on information provided by derivative prices. In conventional GARCH models, the conditional variance depends on lagged returns, such that $h_{t+1} \in \sigma(R_t, R_{t-1}, \dots)$. An indirect implication of the variance risk ratio, $\eta = h_t^*/h_t$, being constant is that h_{t+1}^* is also driven exclusively by lagged returns, and there is no way for derivative pricing to contribute to the dynamic properties of h_{t+1}^* . By permitting η to be time-varying, it becomes possible to incorporate derivative prices in the modeling of h_{t+1}^* . We take advantage of this feature in our empirical implementation.

Second, the structure in Theorem 1 nests the Black-Scholes model as a special case. This classical model arises when h_t and η_t are constant with $\eta_t = 1$, because it leads to the pricing kernel given by the power utility function, see Rubinstein (1976). When η_t is time-varying we have time variation in the risk aversion parameters, which is similar to the habit formation models, see Campbell and Cochrane (1999).

Third, this framework can generate a variety of shapes of the pricing kernel. Based on the empirical estimates of the model, see Section 5, we present the shape of the pricing kernel for two levels of the variance risk ratio, $\eta_{\text{low}} = 0.7$ and $\eta_{\text{high}} = 1.7$, which were chosen to match the 10% and 90% quantile for η_t in our empirical analysis. The upper left panel of Figure 2 displays the shape of the estimated pricing kernel for cumulated returns over one month. The low value of η produce an inverted U -shape similar to that observed during the years 2004 to 2007, whereas the high value of η results in a shape with a pronounced U -shape.

Fourth, the model generates time-varying leverage under \mathbb{Q} , which manifests itself in a number of ways. A time-varying leverage effect will impact the distribution of cumulative returns, and the lower panels of Figure 2 show the skewness and kurtosis of cumulative returns under \mathbb{Q} as a function of days returns are cumulated over (the x -axis). These results are based on 100,000 simulations.⁴ Skewness and kurtosis are shown for the two levels of the variance risk ratio, η_{low} and η_{high} , and these result in distinctively different levels of skewness and kurtosis under \mathbb{Q} . Both skewness and kurtosis are far more pronounced

²The variance risk ratio, η_t , is obviously related to the VRP, which concerns future expectations of $h_{t+1}^* - h_{t+1}$. In the present context, $\log \eta_t$ could serve as a model-based measure of the VRP, as an alternative to the model-free measures by Carr and Wu (2008) and Bollerslev et al. (2011). In Christoffersen et al. (2013) the ratio h_t^*/h_t is held constant. So their time-variation in the VRP is solely driven by the concavity of the logarithm and variation in h_t , and $h_t^* - h_t = (\eta - 1)h_t$.

³Because $\alpha > 0$ in the Heston-Nandi GARCH model.

⁴We simulate using the estimated “SHNG model” based on option prices, see Table 2.

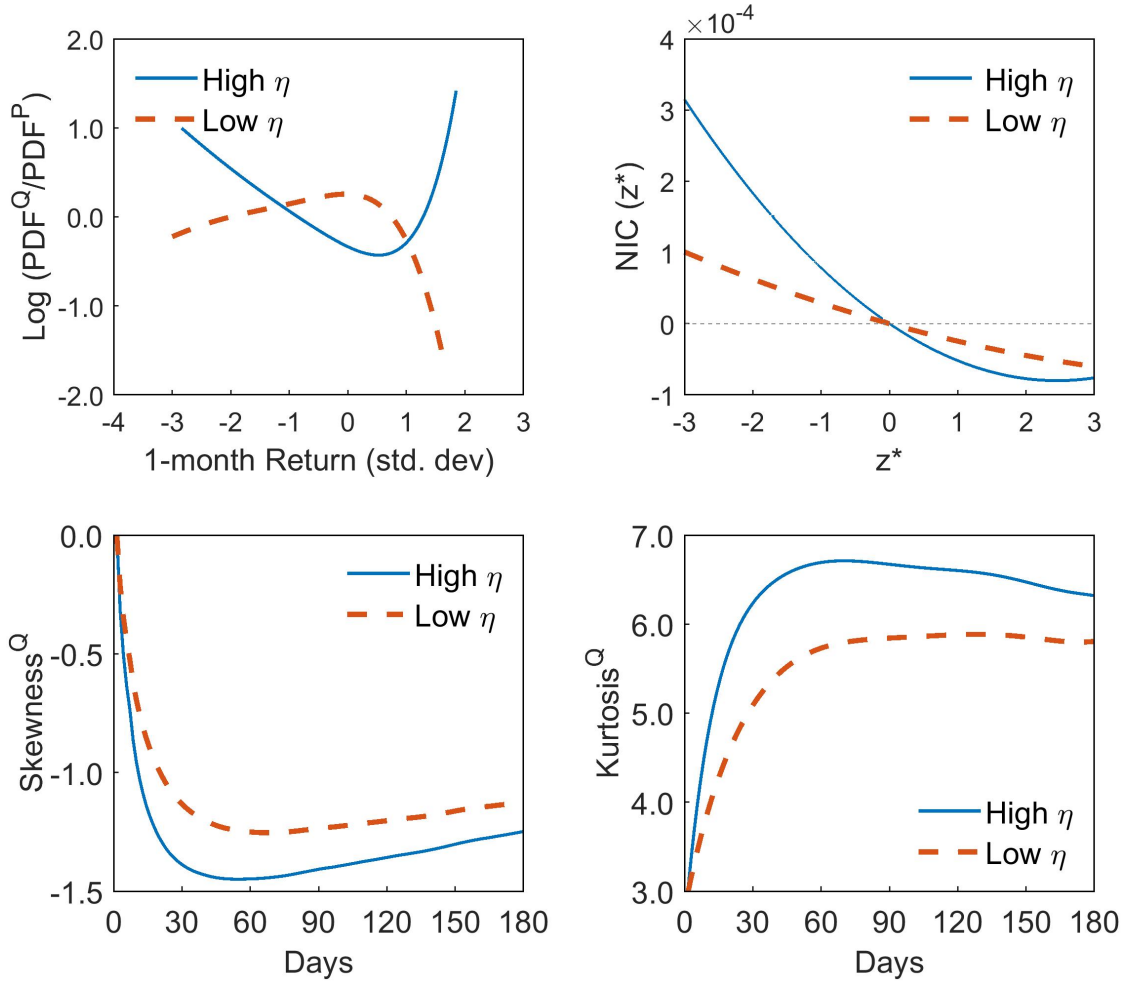


Figure 2: Properties of cumulative returns with a low variance risk ratio, $\eta_{\text{low}} = 0.7$, (dashed lines) and a high variance risk ratio, $\eta_{\text{high}} = 1.7$, (solid lines). The levels correspond to quantiles for η_t in our empirical analysis, the 10% and 90%, respectively. Log-ratios of the \mathbb{Q} -to- \mathbb{P} densities for cumulative returns over one month are shown in the upper left panel, news impact curves under \mathbb{Q} are shown in the upper right panel, and the skewness and kurtosis of multi-period cumulative returns under the risk neutral measure \mathbb{Q} are shown in the two lower panels.

for the large value of η . Another way to illustrate the leverage effect is with the news impact curve by Engle and Ng (1993). The news impact curve under \mathbb{Q} is defined by $\text{NIC}(z^*) = \mathbb{E}_t^{\mathbb{Q}}(h_{t+1}^* | z_t^* = z^*) - \mathbb{E}_t^{\mathbb{Q}}(h_{t+1}^* | z_t^* = 0)$, and from Theorem 1 it follows that

$$\text{NIC}(z^*) = \alpha\eta_t\eta_{t-1}z^{*2} - 2\alpha\gamma\eta_t\sqrt{h_t^*}z^*, \quad (8)$$

whose shape depends on the variance risk ratio. The upper right panel of Figure 2 presents the news impact curve, $\text{NIC}(z^*)$, for the two different level of η , where we evaluate (8) with h_t^* equal to its unconditional mean under \mathbb{Q} , as estimated in Section 5, and with η_t and η_{t-1} equal to either η_{low} (red dashed line) or η_{high} (solid blue line). We observe the asymmetric shape of the news impact curve, see e.g. Chen and Ghysels (2011). However, the level of asymmetry depends on the level of η , such that volatility is far more responsive to negative return shocks when η is high, than when η is small.

3 Derivative Pricing with Dynamic Volatility Risk Aversion

In this section we consider cases where η_t is time-varying. We derive closed-form expression for the VIX under the assumption that $\log \eta_t$ follows an autoregressive process of order one, AR(1). We also derive closed-form expressions for option prices when the path of $\log \eta_t$ is predetermined until maturity date, but otherwise arbitrary. Then we introduce a Taylor expansion of a moment generating function (MGF) that leads to an approximate closed-form expressions for option prices when $\log \eta_t$ follow an AR(1) process.

3.1 VIX Pricing

Once the dynamic properties of η_t are know under \mathbb{Q} , it is relatively straight forward to obtain closed-form expressions for VIX pricing. This only requires expressions for $\mathbb{E}_t^{\mathbb{Q}}(h_{t+k}^*)$, $k = 1, \dots, M$, because the risk-neutral dynamics of returns under Theorem 1 implies the following M -period ahead VIX pricing formula

$$\text{VIX}_t = A \times \sqrt{\frac{1}{M} \sum_{k=1}^M \mathbb{E}_t^{\mathbb{Q}}(h_{t+k}^*)},$$

where $A = 100\sqrt{252}$ is the annualizing factor. The next theorem presents VIX pricing for the case where $\log \eta_t$ is an AR(1) process with i.i.d innovations.⁵

Assumption 3. *Suppose that*

$$\log \eta_t = (1 - \theta)\zeta + \theta \log \eta_{t-1} + \varepsilon_t, \quad (9)$$

where $|\theta| < 1$ and ε_t are i.i.d innovations with $\mathbb{E}^{\mathbb{Q}}(\varepsilon_t | \mathcal{G}_{t-1}) = 0$ and $\text{var}^{\mathbb{Q}}(\varepsilon_t | \mathcal{G}_{t-1}) = \sigma^2 < \infty$.

⁵Extending to the case with ARMA(p, q) process is possible at the expense of less transparent expressions.

Theorem 2 (VIX pricing). *Suppose that Assumptions 1-3 hold. Then the VIX is given by*

$$\text{VIX}(M, \sigma^2, \eta_t, h_{t+1}^*) = \sqrt{a_1(\eta_t, M, \sigma^2) + a_2(\eta_t, M, \sigma^2)h_{t+1}^*}, \quad (10)$$

where $a_1(\eta_t, M, \sigma^2)$ and $a_2(\eta_t, M, \sigma^2)$ are given in Appendix A.2.⁶

In our empirical analysis we find that it is important to account for the stochastic variation in η_t . The parameter, σ^2 , increases the average VIX pricing formulae by 0.97% to 7.47%, for maturities ranging from one to six month. The random variation in η is also important for the variance of cumulative returns, as can be seen in the upper right panel of Figure 4. The first-order approximation, which is based on the future expected path of η_t , but not random variation, in η_t , implies a variance under \mathbb{Q} that is too small, especially for returns cumulated over longer periods. In contrast, the second-order approximation that account for random variation leads to quite accurate values for the annualized variance.

3.2 Option Pricing

In this section we derive the option pricing formula for the case where the variance risk aversion is time-varying. It is important to distinguish between the case where the future path for η_t is predetermined and the case where future values for η_t are stochastic. For an option with M periods to maturity, the vector of relevant path of $\log \eta_t$ is

$$\tilde{\boldsymbol{\eta}}_{t,M} = (\log \eta_{t+1}, \dots, \log \eta_{t+M})',$$

and we denote its expected path by $\tilde{\boldsymbol{\eta}}_{t,M}^e = (\mathbb{E}_t^{\mathbb{Q}}(\log \eta_{t+1}), \dots, \mathbb{E}_t^{\mathbb{Q}}(\log \eta_{t+M}))'$. When η_t is predetermined (i.e. $\sigma^2 = 0$), we have $\tilde{\boldsymbol{\eta}}_{t,M} = \tilde{\boldsymbol{\eta}}_{t,M}^e$ and the affine structure is preserved, such that closed-form option prices formula can be derived from the moments generating function. The VIX pricing formula revealed how uncertainty about future path of $\tilde{\boldsymbol{\eta}}_{t,M}$ is associates with a premium. With stochastic variation in η_t , the option pricing model is no longer affine. However, we can derive an analytical approximation with a suitable Taylor expansion of the MGF of future cumulative returns.

3.2.1 Case with Predetermined Variance Risk Aversion

The option pricing formula for the predetermined case can be deduced from the moments generating function of cumulative returns. This is a relatively straight forward extension of the result with a constant η_t , which is derived in Christoffersen et al. (2013).

When $\tilde{\boldsymbol{\eta}}_{t,M}$ is predetermined, it follows from Theorem 1 that ϕ_t , ξ_t , and the GARCH parameters under \mathbb{Q} , $(\omega_t^*, \alpha_t^*, \beta_t^*, \gamma_t^*)$, are also predetermined. This preserves the affine structure and we can obtain a closed-form pricing formula. We denote this formula by

⁶We have suppressed the terms dependence on θ , ζ , and the parameters of the HNG model and (10) suppresses an approximation term that is negligible in practice (see Lemma A.1).

$C^*(S_t, M, K, r; \tilde{\eta}_{t,M}, h_{t+1}^*)$, where $\tilde{\eta}_{t,M}$ is used as the fourth argument to indicate that the future path of η_t is predetermined. This pricing formula simplifies to that in [Christoffersen et al. \(2013\)](#) in the special case where $\tilde{\eta}_{t,M} = (\log \eta, \dots, \log \eta)$.

Theorem 3. *Suppose that Assumptions 1 and 2 hold and that $\tilde{\eta}_{t,M}$ is predetermined. Then the option pricing formula is given by*

$$C^*(S_t, M, K, r; \tilde{\eta}_{t,M}, h_{t+1}^*) = S_t P_1(t) - K \exp(-rM) P_2(t), \quad (11)$$

where

$$\begin{aligned} P_1(t) &= \frac{1}{2} + \frac{\exp(-rM)}{\pi} \int_0^\infty \operatorname{Re} \left[\frac{K^{-i\varphi} g_{t,M}^*(i\varphi + 1)}{i\varphi S_t} \right] d\varphi, \\ P_2(t) &= \frac{1}{2} + \frac{1}{\pi} \int_0^\infty \operatorname{Re} \left[\frac{K^{-i\varphi} g_{t,M}^*(i\varphi)}{i\varphi} \right] d\varphi, \end{aligned}$$

where the operator $\operatorname{Re}[\cdot]$ takes the real part of the complex number inside the square bracket and $g_{t,M}^*(s) = \mathbb{E}_t^{\mathbb{Q}}(\exp(s \sum_{i=1}^M R_{t+i}))$ is the moments generating function for cumulative returns under \mathbb{Q} . It has the affine form,

$$g_{t,M}^*(s) = \exp(A_T(s, M) + B_T(s, M)h_{t+1}^*), \quad T = t + M,$$

where the expressions for $A_T(s, m)$ and $B_T(s, m)$ are given in the [Appendix A.3](#).

3.2.2 Option Pricing with Stochastic Variance Risk Aversion

We now turn to the more challenging problem where $\tilde{\eta}_{t,M}$ is stochastic. The MGF does not have an affine form when $\sigma > 0$, and this thwarts the standard approach to obtaining a closed-form option pricing formula. It is common to resort to simulation methods in this situation, but we will instead propose a novel method that uses a Taylor expansion of $\tilde{\eta}_{t,M}$ about its conditional expectations, $\tilde{\eta}_{t,M}^e$. This Taylor expansion is used to adjust $g_{t,M}^*(s)$ for the random variation in η_t , and the resulting approximate MGF, $\hat{g}_{t,M}(s)$, can be used to price derivatives in the same way that $g_{t,M}^*(s)$ is used in the predetermined case.

Proposition 1. *Suppose that Assumptions 1-3 hold. The approximate model-implied moments generating function, based on a second-order Taylor expansion, is given by*

$$\hat{g}_{t,M}(s) = g_{t,M}^*(s) \left[1 + \frac{\sigma^2}{2} \operatorname{tr}\{H_{t,M}(s) A_M A_M'\} \right],$$

where $g_{t,M}^*(s)$ are the MGF defined in [Theorem 3](#) with $\tilde{\eta}_{t,M} = \tilde{\eta}_{t,M}^e$ ($\sigma = 0$). The expressions for $H_{t,M}(s)$ and the matrix A_M are given in [Appendix A.5](#).⁷

⁷While $g_{t,M}^*(s)$ is a MGF its approximation, $\hat{g}_{t,M}(s)$, need not be one, because there may not exist a density for which $\hat{g}_{t,M}(s)$ is the corresponding MGF.

Proposition 1 makes it clear how random variation in η_t impacts the MGF, and the predetermined MGF arises as the special case where $\sigma = 0$.

This framework is useful for comparing the three different specification for η_t : Constant, predetermined, and stochastic, and we can interpret the corresponding pricing formulae as being based on Taylor approximations of orders, zero, first, and second, respectively. The second-order approximation accounts for the first two moments of η_t . The first-order approximation accounts for expected path of η_t but not higher order moments, and the we will refer to the case where η_t is taken to be constant, as the zero-order approximation.

The second-order expression presented in Proposition 1 is also the third-order approximation, because the third term is zero under our distributional assumptions, see Appendix A.5.

The first panel in Figure 4 makes a comparison of the true (blue line), first-order approximated (gray dashed line) and second-order approximated (red dashed line) risk-neutral six-month cumulative return density for the score-driven Heston-Nandi GARCH model. The initial conditional variance under \mathbb{P} and variance risk ratio η are all set to their unconditional means. The true density are obtained by simulations, and the two approximated densities are calculated using Fourier inverse transform based on the analytical MGF of cumulative returns. We observe that the second-order approximation fits the true density function very well, but the 1st-order approximation somewhat fails to match the right half part of density function.

To explore the approximation errors for the Taylor expansion more closely, we also plot the (annualized) variance, skewness and kurtosis of multi-period cumulative returns in Figure 4. Note that although it is possible to compute the k -th moment of cumulative returns by evaluating the k -th derivative of the MGF at the point of zero, computing the high-order derivative of MGF given in Proposition 1 is somewhat complicated. Theorem 4 present a more straightforward way by directly calculating an integral. As is evident in Figure 4, omitting the random variation in the variance risk ratio results in a significant lower variance, bigger skewness and smaller kurtosis, and the 2nd-order approximation would greatly mitigate these fitting errors.

Theorem 4. *The risk-neutral k -th moments of cumulative returns can be expressed as*

$$\mathbb{E}_t^{\mathbb{Q}} \left(R_{t,M}^k \right) = \frac{1}{\pi} \int_0^\infty \operatorname{Re} \left[\frac{k!}{v^{k+1}} g_{t,M}(v) - \frac{k!}{u^{k+1}} g_{t,M}(u) \right] ds,$$

where $R_{t,M} = \sum_{i=1}^M R_{t+i}$, and u, v are two complex numbers denoted by $u = u_R + is$ and $v = v_R + is$, with $u_R < 0$, $v_R > 0$ and $s \in \mathbb{R}$. The function, $g_{t,M}(u) = \mathbb{E}_t^{\mathbb{Q}} [\exp(uR_{t,M})]$, is the conditional characteristic function of cumulated returns over M periods.

To the best of our knowledge this result in Theorem 4 is new.

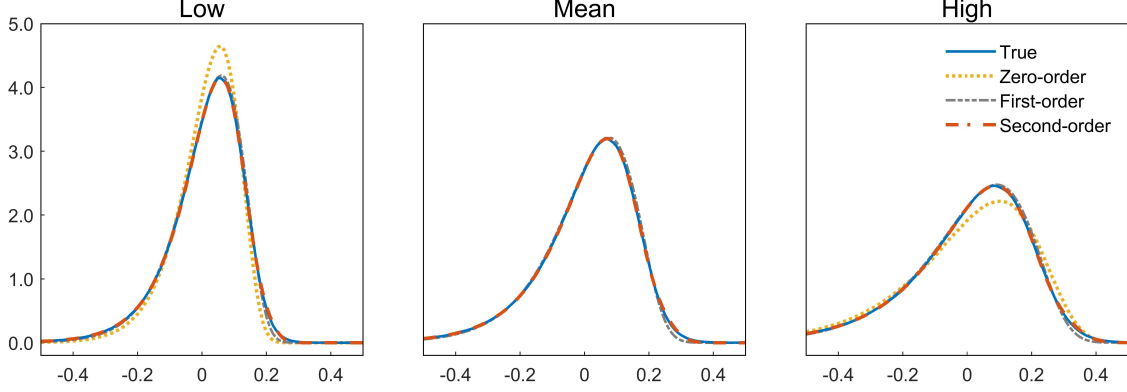


Figure 3: A comparison of the true (solid line), first-order approximated (dashed line) and second-order approximated (dashed-dotted line) six-month risk-neutral cumulative return density for the score-driven Heston-Nandi GARCH model, under different initial value of variance risk ratio η . The initial conditional variance under \mathbb{P} is set to its unconditional mean.

4 Observation-Driven Model for Variance Risk Aversion

In this section, we develop an observation-driven model for η_t , which makes it possible to implement the results of the previous section. In practice, we need to infer the current value of η_t and estimate the dynamic model for η_t . To this end, we adopt an intuitive observation-driven model for η_t , inspired by the score-driven framework by [Creal et al. \(2013\)](#). We use the first-order conditions for minimizing derivative pricing errors to define innovations to η_t , such that η is adjusted to reduce pricing errors (on average).⁸ The first-order condition of the log-likelihood function is presented in the empirical section. At this point, it suffices to express the log-likelihood function in its generic form, $\sum_{t=1}^T \ell(R_t, X_t | \mathcal{F}_{t-1})$, where T is the sample size, and observe that it relies on information from both \mathbb{P} and \mathbb{Q} . We factorize $\ell(R_t, X_t | \mathcal{F}_{t-1}) = \ell(R_t | \mathcal{F}_{t-1}) + \ell(X_t | R_t, \mathcal{F}_{t-1})$, where the latter can be expressed as $\ell_t(X_t | \mathcal{G}_t)$. This likelihood term measures how well the observed derivative prices are explained by the statistical model for returns and the pricing kernel.

A score-driven model updates a parameter in the direction dictated by its first-order conditions of the log-likelihood function, which is known as the score.⁹ The relevant score is $\partial \ell(X_t | \mathcal{G}_t) / \partial \log \eta_t$, because $\ell(R_t | \mathcal{F}_{t-1})$ does not depend on η . The required structure for ε_t , as specified in [Assumption 3](#), motivates the choice

$$\varepsilon_t = \sigma s_{t-1}, \tag{12}$$

⁸Alternatively, one could adopt state space approach. This is computationally more complicated without necessarily providing any benefit. Even when the true model is a state space model, score-driven models are rarely found to be inferior, see [Koopman et al. \(2016\)](#).

⁹The score-driven approach is locally optimal in the Kullback-Leibler sense, see [Blasques et al. \(2015\)](#).

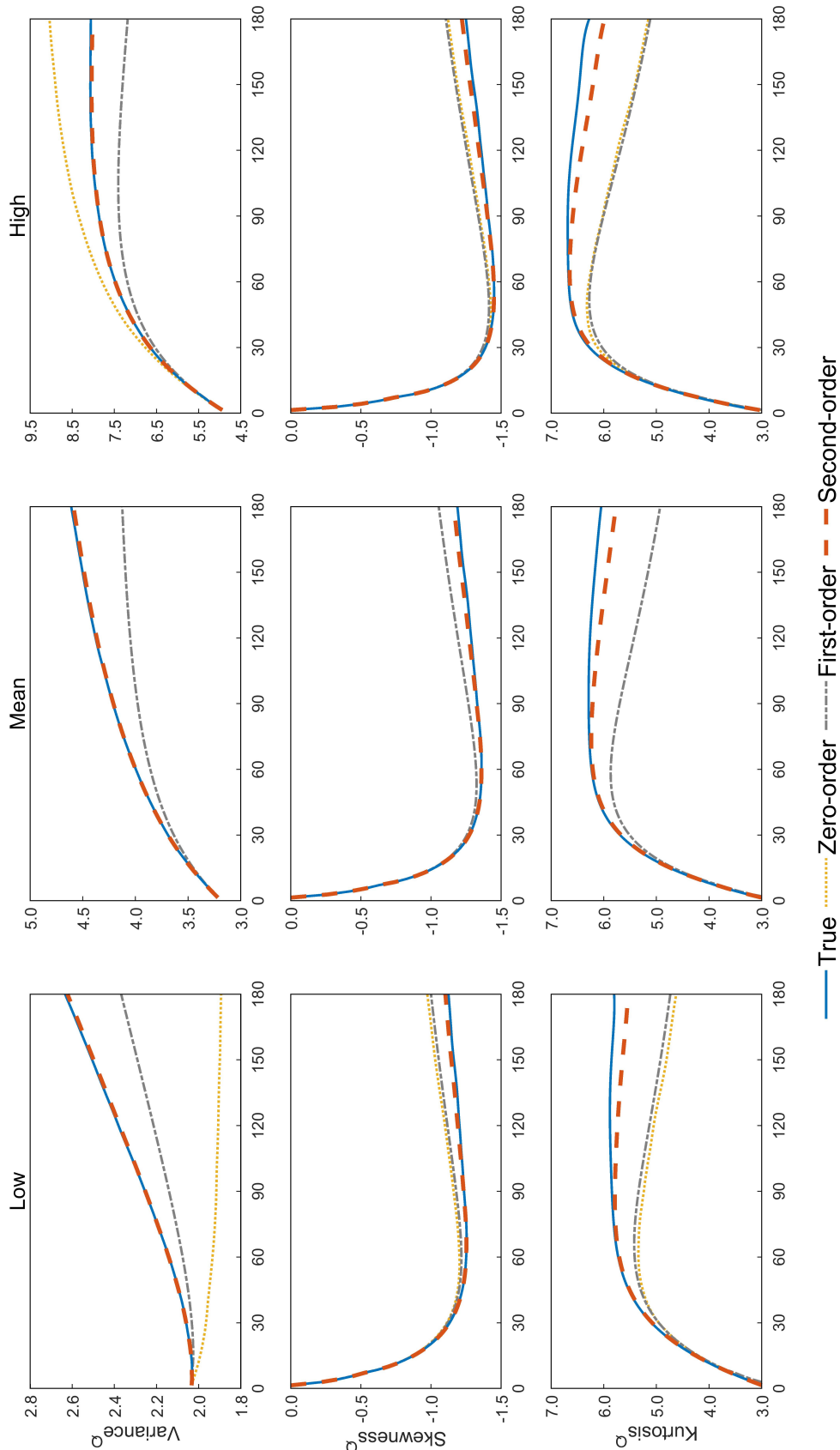


Figure 4: Moments of cumulative returns for different initial variance risk ratios, $\eta_0 = 0.7$ (left panels), $\eta_0 = 1.2$ (middle panels), and $\eta_0 = 1.7$ (right panels). Blue lines represent true moments and red dashed lines are those based on the proposed (second-order) approximation method. The proposed approximation is reasonably accurate and dominates the methods based on first-order (gray dashed line) and zero-order (yellow dashed), which correspond to the assumption that η_t is predetermined and constant, respectively. The true density are obtained by simulating 100,000 paths of the score-driven Heston-Nandi GARCH model using parameter values obtained in our empirical analysis of option prices. annualized variance, defined by $\frac{252}{M} \text{Var}_t^{\mathbb{Q}} \left(\sum_{i=1}^M R_{t+i} \right) \times 100\%$, skewness and kurtosis of multi-period cumulative returns are shown. The initial conditional variance under \mathbb{P} is set to its unconditional means.

where the normalized score is defined by

$$s_t = \frac{\nabla_t}{\sqrt{\mathbb{E}^{\mathbb{P}}[\nabla_t^2|\mathcal{G}_t]}}, \quad \text{with} \quad \nabla_t = \frac{\partial \ell(X_t|\mathcal{G}_t)}{\partial \log \eta_t}. \quad (13)$$

When the score is evaluated at the true parameters we have

$$\mathbb{E}^{\mathbb{P}}[s_t|\mathcal{G}_t] = 0, \quad \text{and} \quad \text{var}^{\mathbb{P}}[s_t|\mathcal{G}_t] = 1,$$

such that $\mathbb{E}^{\mathbb{P}}[\varepsilon_t|\mathcal{G}_{t-1}] = 0$ and $\text{var}^{\mathbb{P}}[\varepsilon_t|\mathcal{G}_{t-1}] = \sigma^2$, since s_t is \mathcal{F}_t -measurable. Note that this definition of score does not ensure that $\{s_t\}$ is a sequence of i.i.d. random variables. This requires additional assumptions about the pricing errors, such as that made in Assumption 4 that implies that s_t i.i.d. and standard normally distributed, see Theorem 5 below. From (9) and the specification (12) it follows that the variance risk ratio, η_t , is \mathcal{F}_{t-1} -measurable, and this ensures that information about derivatives prices are not used to price themselves.

This approach to modeling $\log \eta_t$ is analogous to the way the conditional variance is modeled in GARCH models. For instance, the GARCH(1,1) model by Bollerslev (1986) has, $h_t = c + bh_{t-1} + a(r_{t-1}^2 - h_{t-1})$, such that changes in h_t are driven by discrepancies between squared returns and the conditional variance. The score model invokes a similar self-adjusting property, where $\log \eta_t$ is updated whenever the derivative prices indicates a that a different value of $\log \eta_t$ would result in smaller pricing errors.

This score-drive approach could be adopted with more general specifications for $\log \eta_t$, than the AR(1) model we have used here. For instance, could include exogenous variables and lagged endogenous variables as explanatory variables, or used a long-memory specification for $\log \eta_t$. A main challenge to alternative specification is that the derivative prices formulae would need to be established first. Such extensions might be possible for the VIX, but would be challenging for option pricing in general. The score-driven approach used here, can also be based on first order conditions for other criteria such as a loss functions.

4.1 The Log-Likelihood Function and the Form of Score

Next we turn to the log-likelihood functions that is used to estimated model parameters. Our observed data consist of returns, R_t , and a vector of derivative prices, X_t , and we can, without loss of generality, factorize the log-likelihood function as follows,

$$\ell(R_1, \dots, R_T, X_1, \dots, X_T, \mathcal{F}_0) = \sum_{t=1}^T \ell(R_t, X_t|\mathcal{F}_{t-1}) = \sum_{t=1}^T \ell(R_t|\mathcal{F}_{t-1}) + \ell(X_t|R_t, \mathcal{F}_{t-1}). \quad (14)$$

This decomposition was also used in Christoffersen et al. (2013). The log-likelihood function for returns, $\ell(R_t|\mathcal{F}_{t-1})$, is given from the HNG model and the assumption that return shocks

are iid Gaussian distributed, $z_t \sim iid N(0, 1)$. Thus,

$$\ell(R_t|\mathcal{F}_{t-1}) = -\frac{1}{2} \left[\log(2\pi) + \log h_t + (R_t - r - (\lambda - \frac{1}{2})h_t)^2/h_t \right].$$

To complete the model, we need to specify the log-likelihood function for the vector of derivative prices, X_t , $\ell(X_t|R_t, \mathcal{F}_{t-1}) = \ell(X_t|\mathcal{G}_t)$. To this end, we let $X_t^m \in \mathcal{G}_t$ denote the vector of model-based prices and make following assumptions for pricing errors.

Assumption 4. *The derivatives pricing errors follow a multivariate normal distribution*

$$e_t = X_t - X_t^m \sim iid N \left(0, \sigma_e^2 \Omega_{N_t} \right),$$

with correlation matrix Ω_{N_t} , where N_t is the number of derivative prices at times t .

The vector of “prices”, X_t , can be defined in a number of ways. Wang et al. (2017) measures X_t in the unit of volatility (the level of VIX), Christoffersen et al. (2013) use the Vega-weighted option prices, and Feunou and Okou (2019) use the Black-Scholes implied volatility. In our empirical analysis we used the logarithmically transformed VIX and logarithmically transformed Black-Scholes implied volatilities for options. This is the natural in the score-driven model for $\log \eta_t$ and this choice is less likely to induced severe misspecification, because the distribution of the log-volatilities are well approximated by a Gaussian distribution, see Andersen et al. (2003).

Existing empirical studies are based on the assumption that pricing errors are uncorrelated, which corresponds to the correlation matrix being the identity matrix, $\Omega_{N_t} = I_{N_t}$. This is an unrealistic assumption because contemporaneous pricing errors tend to be positively correlated. Assumption 4 allows for a common correlation and this is important for the statistical properties of the definition of the score, see Theorem 5 below. For instance, in our empirical analysis with option prices the misspecification resulting from imposing $\Omega_{N_t} = I_{N_t}$ would induce an upwards bias in the estimated variance of s_t .

Assumption 5. *Based on Assumption 4, the pricing errors for options are approximately distributed with an equicorrelation matrix, given by $\Omega_{N_t} = \rho + (1 - \rho)I_{N_t}$.*

Assuming a common correlation for pricing errors is particularly useful whenever the panel of derivatives prices is unbalanced over time, because it makes the time-varying dimension of, Ω_{N_t} , unproblematic. A common correlation can be motivated by the structure where the option pricing errors are given by, $e_{i,t} = u_t + v_{i,t}$, where u_t is a common term and $v_{i,t}$, $i = 1, \dots, N_t$ are uncorrelated idiosyncratic terms. This will bring about the structure in Assumption 5, where $\rho = \sigma_u^2 / (\sigma_u^2 + \sigma_v^2)$ and $\sigma_e^2 = \sigma_u^2 + \sigma_v^2$.

Under Assumption 4, the part of the log-likelihood function that is related to derivative prices is

$$\ell(X_t|\mathcal{G}_t) = \ell(X_t|\mathcal{G}_t) = -\frac{1}{2} \left(N_t \log(2\pi\sigma_e^2) + \log |\Omega_{N_t}| + \sigma_e^{-2} e_t' \Omega_{N_t}^{-1} e_t \right). \quad (15)$$

A related virtue of the way we have introduced time-variation in the pricing kernel, is that the model (for returns) under the physical measure continues to be a time-homogeneous Heston-GARCH model, that does not depend on derivative prices. So the parameters in the model could, if needed, be estimated by two-stage estimation methods, where the parameters in the GARCH model is estimated from returns in a first stage, while the remaining parameters are estimated in a second stage using derivative prices.¹⁰

Theorem 5. *Suppose that Assumption 4 hold, then score defined in (13) is given by*

$$\nabla_t = \frac{1}{\sigma_e^2} \left(\frac{\partial X_t^m}{\partial \log \eta_t} \right)' \Omega_{N_t}^{-1} e_t$$

with conditional variance

$$\mathbb{E}^{\mathbb{P}}[\nabla_t^2 | \mathcal{G}_t] = \frac{1}{\sigma_e^2} \left(\frac{\partial X_t^m}{\partial \log \eta_t} \right)' \Omega_{N_t}^{-1} \left(\frac{\partial X_t^m}{\partial \log \eta_t} \right),$$

and the scaled score is *i.i.d* standard normally distributed, both in \mathbb{P} and \mathbb{Q} measures

$$s_t = \frac{\nabla_t}{\sqrt{\mathbb{E}^{\mathbb{P}}[\nabla_t^2 | \mathcal{G}_t]}} \sim \text{i.i.d } N(0, 1).$$

To obtain the score, we need to derive $\partial X_t^m / \partial \log \eta_t$, which must be done separately for the VIX and option prices. These terms are derived in Appendix A.6.1 and Appendix A.6.2, respectively. The scaled score simplifies to

$$s_t = \frac{1}{\sigma_e} \text{sign} \left(\frac{\partial X_t^m}{\partial \log \eta_t} \right) e_t,$$

in the special case where X_t^m is univariate, i.e. the case with a single derivative. From this expression it is evident that score will indicate the direction for η , which is expected to led to smaller pricing errors.

5 Empirical Analysis

5.1 Data

Our empirical analysis is based on daily returns for the S&P 500 index, the CBOE VIX, and option prices on the exchange traded fund, SPX, that tracks the S&P 500 index. Our sample period spans 32 years from January 2nd, 1990 to December 31, 2021 with 8,064 trading days. Returns are defined from cum-dividend logarithmic transformed closing prices, which were

¹⁰We used joint estimation as it because straight forward and did not cause any computational issues. Two-stage estimation can greatly reduce the computational burden, and is often used in this context, see e.g. Broadie et al. (2007), Corsi et al. (2013), Christoffersen et al. (2013) and Majewski et al. (2015), and two-stage estimation could be implemented for our model, if computational considerations required it.

downloaded from the Wharton Research Data Services (WRDS). Daily VIX prices were downloaded from the website of the Chicago Board Options Exchange (CBOE). The SPX option prices were obtained from two sources. Prices for the first six year years (1990–1995) are the so-called Optsum data, which were purchased from CBOEs website. Option prices for the remaining 26 years are OptionMetrics data downloaded from the WRDS database. Option prices were preprocessing following [Christoffersen et al. \(2014\)](#) and [Bakshi et al. \(1997\)](#). Specifically, we include out-of-the-money put and call option prices with positive trading volume and with maturity between two weeks and six months, and put option prices are converted to in-the-money call options using the put-call parity. Much of the existing literature use weekly data. A panel of option prices is typically sampled on Wednesdays, because liquidity tends to be highest on Wednesdays. In our analysis, we use daily option prices, because a daily score, s_t , is needed to update η_t . The number of available options has grown rapidly over the sample period in terms of the available maturities and the available moneyness at each maturity.¹¹ From the pool of available options we select (as many as) six options per trading day. The selection is done as follows: For each of the available maturities on day t , we admit the most liquid option as measured by daily trading volume. The admitted options are sorted by maturity in ascending order, and indexed by $j = 1, \dots, \tilde{N}_t$, where \tilde{N}_t is the number of distinct maturities on day t . From this set, we include all of them if $\tilde{N}_t \leq 6$, we include the first six if $7 \leq \tilde{N}_t \leq 10$, we include $\{1, 3, 5, 7, 9, 11\}$ if $11 \leq \tilde{N}_t \leq 15$, we include $\{1, 4, 7, 10, 13, 16\}$ if $16 \leq \tilde{N}_t \leq 20$, and so forth. This gives us a set with N_t options every day that include a representative range of the available maturities. This procedure yields $N_t = 6$ options on most days, and the total number of option prices in our sample period is 37,152.

Table 1 contains descriptive statistics for our S&P 500 returns and the VIX in Panel A and option prices in Panel B. As expected, the sample average of the VIX (19.48%) is larger than the standard deviation for annualized returns (18.11%). Their difference reflects the (average) negative volatility risk premium. The S&P 500 returns exhibit a small negative skewness and a high degree of kurtosis, whereas the the VIX has positive skewness and a large kurtosis. We also report summery statistics for option prices partitioned by moneyness, maturity, and the contemporaneous level of VIX. Moneyness is defined by the Black-Scholes delta. Options with delta below 0.5 are out-of-the-money call options, and options with delta above 0.5 are based on the out-of-the-money put options. Deep out-of-the-money put options (i.e. deltas larger than 0.7) are expensive relative to out-of-the-money call options, which reflects the well-known volatility smirk. The implied volatility has a relatively flat term structure with respect to the time to maturity. Unsurprisingly, the implied volatility is increasing in the VIX level, as shown in the bottom of Table 1, where option prices are partitioned by the contemporaneous VIX level.

¹¹The number of available option prices has increased almost 50-fold over our sample period, initially from about 38 daily option prices to well over 1,700.

Table 1: Summary Statistics

<i>A: S&P 500 returns and and CBOE VIX</i>					
	Mean(%)	Std(%)	Skewness	Kurtosis	Obs.
Returns (annualized)	8.13	18.11	-0.41	14.37	8,064
VIX	19.48	8.01	2.21	11.49	8,064
<i>B: Option Price Data</i>					
	Implied Volatility (%)	Average price (\$)	Observations		
All options	18.47	63.63	37,152		
<i>Partitioned by Moneyness</i>					
Delta<0.3	14.18	11.04	5,452		
0.3≤Delta<0.4	15.52	20.92	2,955		
0.4≤Delta<0.5	16.76	33.92	3,912		
0.5≤Delta<0.6	18.94	48.78	7,091		
0.6≤Delta<0.7	19.40	64.86	6,098		
0.7≤Delta	21.02	117.47	11,644		
<i>Partitioned by Maturity</i>					
DTM<30	16.89	41.41	9,614		
30≤DTM<60	17.91	52.29	9,696		
60≤DTM<90	19.00	65.63	7,465		
90≤DTM<120	20.25	87.43	4,421		
120≤DTM<150	20.22	98.51	2,931		
150≤DTM	19.68	97.06	3,025		
<i>Partitioned by the level of VIX</i>					
VIX<15	12.15	44.77	12,638		
15≤VIX<20	16.70	62.49	10,788		
20≤VIX<25	21.45	74.72	7,143		
25≤VIX<30	25.43	84.16	3,395		
30≤VIX<35	29.61	88.12	1,456		
35≤VIX	40.23	101.70	1,732		

Note: Summary statistics for close-to-close S&P 500 index returns, VIX and option prices from January 1990 to December 2021. The reported statistics for S&P 500 and VIX index include the sample mean (Mean), standard deviation (Std), skewness (Skew), kurtosis (Kurt), number of observations (Obs). Option prices are based on closing prices of out-of-the-money call and put options. We report the average Black-Scholes implied volatility (IV), average price, and the number of option prices for different partitions of option prices. “Moneyness” is defined by the Black-Scholes delta. DTM denotes the number of calendar days to maturity. Data sources: S&P 500 returns from WRDS, VIX from CBOE’s website. Option prices: Optsum data (1990–1995) and OptionMetrics (1996–2021).

5.2 Parameter estimation

We estimate the model with both constant (CHNG) and time-varying (SHNG) variance risk aversion. Both specifications are estimated with two types of derivative prices, VIX data and the panel of option prices, such that we have four estimated specifications. Parameters are estimated by maximizing the joint log-likelihood function for the full sample period from the beginning of January 1990 to the end of December 2021. Each column reports the parameter estimates for the specification listed in the first row of Table 2. CHNG refers to the model proposed in [Christoffersen et al. \(2013\)](#) and SHNG is the score-driven model proposed in this paper. The entries in brackets, [VIX] and [Opt], identify the type of derivatives used for estimation, VIX and option prices, respectively. Robust standard errors are given in parentheses below the estimates.¹² We also report the implied persistence of volatility under both \mathbb{P} and \mathbb{Q} . These are given by $\pi^{\mathbb{P}} = \beta + \alpha\gamma^2$ and $\pi^{\mathbb{Q}} = \mathbb{E}^{\mathbb{Q}}[\beta_t^* + \alpha_t^*\gamma_{t-1}^{*2}]$, respectively, where the latter simplifies to $\pi^{\mathbb{Q}} = \beta^* + \alpha^*\gamma^{*2}$ for the CHNG model with constant parameter. We also report the different terms of the log-likelihood (for returns and different sets of derivative prices). Some of these likelihood terms can be interpreted as pseudo out-of-sample log-likelihood values and we have indicated these with italic font. For instance the CHNG[VIX] model is estimated using returns and the VIX, but the estimated model also yields model-based option prices that can be compared with actual option prices. The reported log-likelihood for option prices is evaluated with the resulting option pricing errors, that are implicitly used to obtain estimates of ρ and σ_e for option prices. Similarly, we evaluate the log-likelihood for VIX pricing errors for the specifications that were estimated with options prices. In this case we just need to compute the implied estimate of σ_e for VIX prices. The largest log-likelihood within each row is highlighted with bold font.

There are several interesting observations to be made from the estimates in Table 2. First, the volatility process is found to be highly persistent across all specifications, and the persistence is generally larger under the risk-neutral measure than under the physical measure. This is consistent with the existing literature. Second, the equity premium parameter, λ , is estimated to be positive and is significant in all specification. Third, the variance risk ratio, η_t , is typically larger than one. It is significantly larger than one in both CHNG specifications. Similarly, for the SHNG model the expected value of η_t (denoted $\mathbb{E}\eta$) is inferred from the AR(1) model for $\log \eta_t$, and it is also significantly larger than one in both SHNG specifications. The implication is that the risk neutral volatility, h^* , is (on average) larger than the physical volatility, h . Fourth, the parameter that define the leverage effects, γ , is also found to be significant across all specification. Fifth, for the SHNG specification we note that the variance risk ratio, η_t , is highly persistent, because θ is estimated to be close to one. In fact, it is estimated to be more persistent than h_t and h_t^* , across all SHNG specifications. Sixth, the coefficients, σ , that measures the impact that s_{t-1} has

¹²Following [Christoffersen et al. \(2013\)](#), we impose $\omega = 0$ in estimation because the non-negativity constraint, which ensures positive variances, is binding.

Table 2: Joint Estimation Results

Model	CHNG [VIX]	CHNG [Opt]	SHNG [VIX]	SHNG [Opt]
λ	3.377 (1.225)	2.828 (0.022)	3.398 (1.186)	3.088 (0.644)
β	0.902 (0.009)	0.713 (0.008)	0.720 (0.008)	0.570 (0.015)
$\alpha(\times 10^{-6})$	1.166 (0.088)	2.495 (0.012)	4.428 (0.496)	5.833 (0.256)
γ	272.45 (13.95)	326.29 (3.81)	220.45 (11.70)	249.59 (10.28)
ζ			0.192 (0.004)	0.102 (0.0011)
θ			0.988 (0.003)	0.994 (0.001)
σ			0.061 (0.006)	0.042 (0.010)
ρ		0.822 (0.015)		0.087 (0.010)
σ_e	0.175 (0.011)	0.229 (0.024)	0.043 (0.032)	0.091 (0.036)
$\eta, \mathbb{E}\eta$	1.371 (0.041)	1.252 (0.013)	1.314	1.190
$\widehat{\text{var}}(s_t)$			1.000	1.007
$\pi^{\mathbb{P}}$	0.989	0.979	0.935	0.934
$\pi^{\mathbb{Q}}$	0.991	0.983	0.944	0.944
LogL				
$\ell(\text{R})$	26,324	26,419	26,450	26,438
$\ell(\text{VIX})$	2,619	1,612	13,917	7,932
$\ell(\text{Opt})$	15,177	21,647	27,857	36,682
$\ell(\text{R}, \text{VIX})$	28,944	28,031	40,367	34,370
$\ell(\text{R}, \text{Opt})$	41,501	48,067	54,307	63,120

Note: Estimation results for the full sample period (January 1990 to December 2021). Model specifications, CHNG and SHNG, refer to the model by [Christoffersen et al. \(2013\)](#) and the model introduced in this paper, respectively. In brackets, below the model acronyms, we have listed the type of derivative data that was used in the estimation, VIX or option prices. Parameter estimates are reported with robust standard errors (in parentheses), $\pi^{\mathbb{P}}$ and $\pi^{\mathbb{Q}}$ refer to the volatility persistence under \mathbb{P} and \mathbb{Q} , respectively. The value each component of the log-likelihood function is reported in the bottom of the table, where the largest log-likelihood within each row is indicated with bold font.

on η_t , is estimated to be positive and significant. The implied unconditional variance for η_t is similar for the two SHNG specifications, $\text{var}(\eta_t) = 0.29$ when estimated with VIX and $\text{var}(\eta_t) = 0.23$ when estimated with option prices.¹³ Seventh, all specifications yield similar likelihood values for the returns. This is to be expected because they all rely on the Heston Nandi GARCH model for returns. Eighth, the key difference between the CHNG and SHNG models is the enhanced flexibility in SHNGs pricing kernel. This generalization leads to large improvements in the likelihood for derivative prices. This reason is that the adaptive pricing kernel with time-varying variance risk aversion yields model implied derivative prices that are much closer to observed prices, and the substantial reduction in the pricing errors translates to much higher values of the log-likelihood for derivative prices.

Ninth, estimating the models with VIX or option prices results in some differences across the estimated parameters. This is to be expected, since the vector of option prices contains more information (about future returns) than the VIX also. For instance, the leverage parameter, γ , is estimated to be larger with option prices than with the VIX.

Tenth, the correlation between option pricing errors is estimated to be positive and significant for both models. The estimate has the staggering large value of 82.2% for the CHNG model and the more moderate value of 8.7% for SHNG model. Ignoring this correlation (assuming it to be zero) would greatly underestimate the condition variance of $\partial\ell(X_t|R_t, \mathcal{F}_{t-1})/\partial\log\eta_t$, which makes the variance of s_t larger than one.

Figure 5 presents the estimated time series of the variance risk ratio, $\eta_t = h_{t+1}^*/h_{t+1}$, based on the VIX (blue line) and option prices (red line). The two have a high degree of comovement and, as we discussed earlier, the unconditional variance of the two series is very similar. Importantly, the variance risk ratio occasionally falls below one, as is seen during the years: 1993-1995, 2004-2007, and 2017. A value below one, $\eta_t < 1$, means that investors have an increased appetite for variance risk, whereas a large value of η implies that investors demand additional compensation for variance risk. The latter was particularly the case during the financial crises in the immediate aftermath of the Lehman collapse or the recent COVID-19 pandemic. The conditional variance was unusually high during this period under physical measure. The large value for η_t during this period magnifies the impact on h_t^* , so that it increased even more, and to a level that was more than twice that of h_t . The level of η_t based on VIX tend to be slightly larger than that based on option prices. Since these VIX is based on options with 30 days to maturity, whereas our option have maturity with as much as 180 days to maturity. A possible explanation is that short-term investors demanding demands larger compensation for variance risk than long(er)-term investors. This would be consistent with the findings in Eisenbach and Schmalz (2016) and Andries et al. (2018).

¹³The variance for η_t is computed from AR(1) parameters for $\log\eta_t$ and the assumptions that imply that the unconditional distribution for η_t is log-normal.

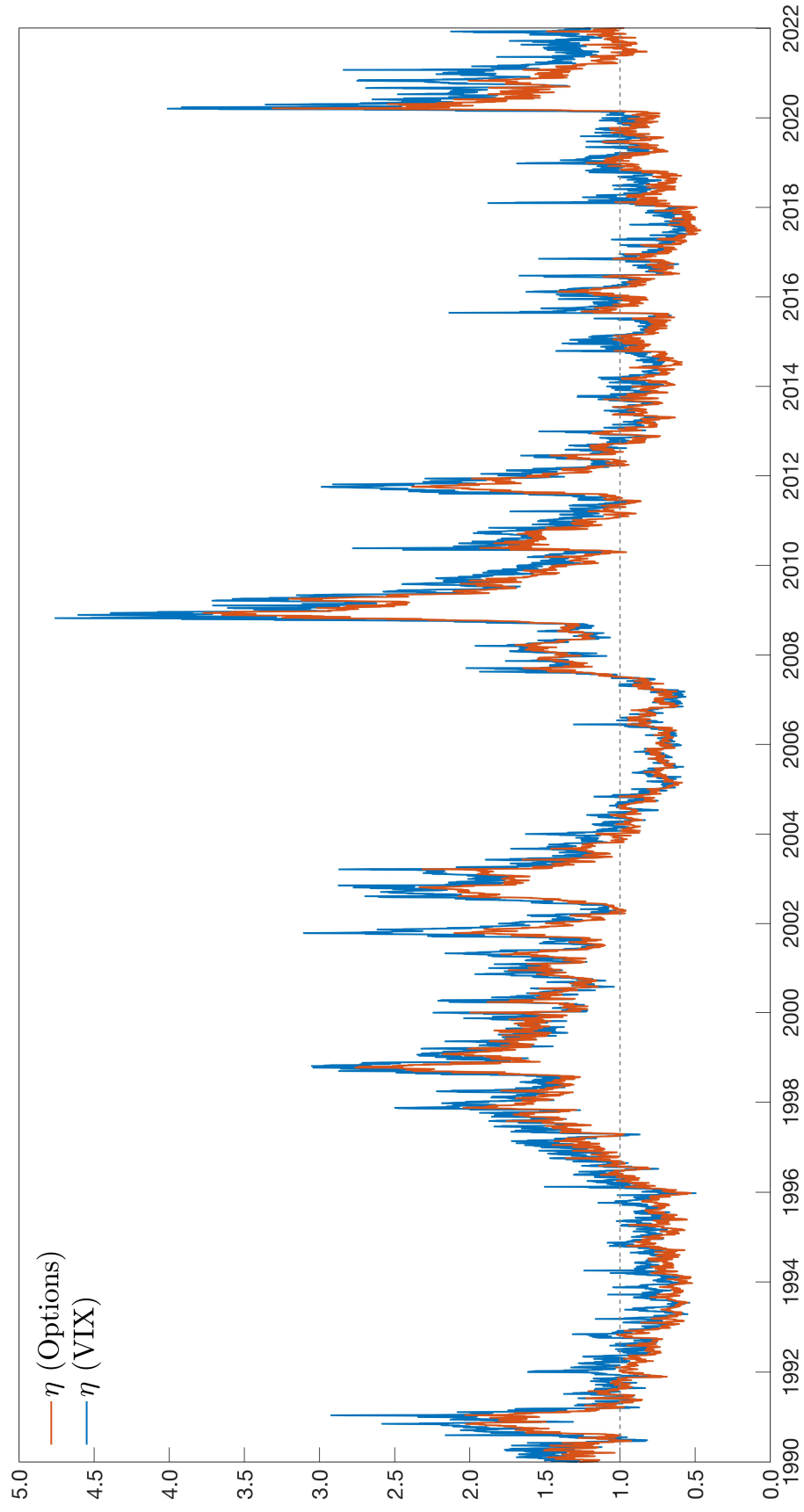


Figure 5: This figure presents time series of the estimated variance risk ratio, η_t . The blue line is based on the VIX and the red line on option prices. The two time series are very similar, albeit the η_t based on the VIX tend to be slightly larger than that based on option prices.

Table 3: VIX and Option Pricing Performance

Model	CHNG [VIX]	CHNG [Opt]	SHNG [VIX]	SHNG [Opt]
<i>A: RMSE for VIX Pricing</i>				
Full Sample	17.49	19.81	4.308	9.049
<i>B: RMSE for Option Pricing</i>				
Full Sample	23.06	22.88	13.34	9.191
<i>Partitioned by moneyness</i>				
Delta<0.3	33.05	29.80	21.11	12.77
0.3≤Delta<0.4	27.84	26.59	17.86	11.28
0.4≤Delta<0.5	23.29	23.87	14.68	9.375
0.5≤Delta<0.6	19.74	21.49	11.41	7.271
0.6≤Delta<0.7	18.83	20.62	9.72	6.859
0.7≤Delta	19.50	19.48	8.78	8.634
<i>Partitioned by maturity</i>				
DTM<30	25.48	23.51	13.72	12.19
30≤DTM<60	23.48	23.27	12.80	7.848
60≤DTM<90	21.78	22.30	12.75	6.914
90≤DTM<120	20.47	21.81	13.51	7.963
120≤DTM<150	20.74	21.68	13.84	8.622
150≤DTM	22.18	23.58	14.45	9.226
<i>Partitioned by the level of VIX</i>				
VIX<15	29.25	28.06	15.60	10.02
15≤VIX<20	18.47	19.72	13.16	9.021
20≤VIX<25	18.23	19.51	10.89	8.224
25≤VIX<30	18.74	18.52	11.02	8.518
30≤VIX<35	19.48	19.23	10.97	8.542
35≤VIX	25.36	22.41	11.57	9.508

Note: This table reports the in-sample VIX and option pricing performance for each model in Table 2. We evaluate the model's option pricing ability through the root of mean square errors of log implied volatility ($RMSE_{IV}$). We summarize the results by option moneyness, maturity and market VIX level. Moneyness is measured by Delta computed from the Black-Scholes model. DTM denotes the number of calendar days to maturity. The numbers in bold indicate the minimum value within each row in each time period.

5.3 In-Sample VIX and Option Pricing Performance

We evaluate and compare the performance of the models in terms of VIX and option pricing. Consistent with the loss function (4) used in the joint MLE, we report pricing errors under the root-mean-squared errors (RMSE) for logarithm of VIX or implied volatilities¹⁴. A similar loss function was adopted in [Ornthanalai \(2014\)](#) who used relative implied volatility as error structure to avoid excessive weighting to data with high volatility levels. The (in-sample) RMSEs are reported in [Table 3](#) for each of the specifications listed in [Table 2](#).

We present the in-sample RMSEs for VIX pricing in Panel A. These are defined by

$$\text{RMSE}_{\text{VIX}} = \sqrt{\frac{1}{T} \sum_{t=1}^T [\log \text{VIX}_t^m - \log \text{VIX}_t]^2} \times 100,$$

where VIX_t^m is model-based and VIX_t is the observed market VIX. Panel A shows that a time-varying variance risk ratio result in substantially smaller average pricing errors, relative to the CHNG models which all assume η to be constant. The improvements in VIX prices that are achieved by permitting time-variation in η are substantial and impressive. The specification that delivers the most accurate VIX pricing is the SHNG model that is estimated with VIX data. It reduces the RMSE by a factor of four relative to the two CHNG specifications. Even the SHNG model that is solely estimated with option prices, has a much lower RMSE for VIX prices than the CHNG specification that is estimated to target VIX pricing. The SHNG models estimated with option prices involves an objective that must price options with maturities ranging from one to six months. This entails a trade-off across maturities, whereas the VIX specification specifically targets a one-month maturity.

In Panel B of [Table 3](#) we report the in-sample performance for option pricing. We follow the literature and convert option prices to their corresponding implied volatilities, as defined by the Black–Scholes formula. We compare the model-based implied volatility, IV^m , with the market-based implied volatility, IV , where the latter is defined by the observed option price. The resulting RMSE,

$$\text{RMSE}_{\text{IV}} = \sqrt{\frac{1}{\sum_{t=1}^T N_t} \sum_{t=1}^T \sum_{i=1}^{N_t} [\log \text{IV}_{t,i}^m - \log \text{IV}_{t,i}]^2} \times 100,$$

is reported the first row of Panel B in [Table 3](#). We also compute the RMSE_{IV} for option partitioned by the characteristics: Moneyness, Time to maturity, and the contemporaneous volatility index level. The resulting RMSEs can be used to identify shortcomings in a model, such as its inability to: generate sufficient leverage effect; capture the dynamic properties; and generate a proper variance risk premium. The smallest RMSE within each row is highlighted with boldface.

¹⁴In [Appendix B](#), we also report the RMSE for VIX or implied volatilities as robustness check.

The SHNG specifications clearly dominate the CHNG specifications in terms of option pricing. The average option pricing errors are substantially better for than the CHNG models, and the smallest RMSE is obtained by the SHNG, which is estimated with option prices. Its RMSE is less than half that of any of the CHNG specifications. Impressively, the SHNG specifications uniformly dominates all CHNG specifications for either VIX or option pricing, across all partitions. This further supports the advantage of allowing for time variation in the variance risk ratio. We note that the largest gains in pricing accuracy are found during periods with low volatility and out-of-the-money call options, which tends to be options with low variance risk premia.

Interestingly, [Christoffersen et al. \(2013\)](#) also estimated an ad-hoc model where the ratio of volatility under \mathbb{P} and \mathbb{Q} is not held constant. This model was used as a benchmark for the CHNG model they proposed in their paper. The ad-hoc model consisted of two separate Heston-GARCH models, one that was fitted to returns under \mathbb{P} , and one that was estimated with option prices under \mathbb{Q} . This model is referred to as ad-hoc, because it makes no attempt to uncover a pricing kernel that can explain the differences between \mathbb{P} and \mathbb{Q} . Moreover, their ad-hoc model did not improve on option pricing relative to the CHNG model with a variance-dependent pricing kernel. Our [Theorem 1](#) offers a theoretical explanation for the poor performance of their ad-hoc models, because [Theorem 1](#) shows a time-varying risk premium is incompatible with Heston-Nandi models that have time-invariant parameters under both \mathbb{P} and \mathbb{Q} .¹⁵

In the next section we evaluate if the substantial in-sample improvements in derivative pricing also holds out-of-sample.

5.4 Out-of-Sample Pricing Performance

In this section we turn to out-of-sample comparisons. The SHNG specification with time-varying η_t is obviously a more flexible model than the CHNG model. Because the SHNG model has additional parameters, its better in-sample performance could potentially be driven by overfitting. It is therefore interesting to investigate if the SHNG model also yields more accurate derivative prices in out-of-sample comparisons. We divide the full dataset into two subsamples. Data from the years 1990-2007 (in-sample) are used to estimate each of the four specifications, whereas data from the period 2008-2021 (out-of-sample) are used to evaluate the estimated models. Analogous to the in-sample comparisons, we evaluate and compare the models in terms of their average root mean squared pricing errors.

The out-of-sample performance by the SHNG model is just as impressive as its in-sample performance. The best VIX pricing is again achieved with SHNG model estimated with VIX and the best option pricing is again achieved by the SHNG model estimated with option

¹⁵The ad-hoc model is therefore internally inconsistent. Moreover, the ad-hoc model only leads to a minuscule improvement in the empirical fit, since the log-likelihood for option prices only improves by about 0.1 units.

Table 4: Out-of-sample VIX and Option Pricing

Model	CHNG [VIX]	CHNG [Opt]	SHNG [VIX]	SHNG [Opt]
<i>A: RMSE for VIX Pricing</i>				
Full Sample	18.33	19.60	4.782	10.03
<i>B: RMSE for Option Pricing</i>				
Full Sample	24.33	20.98	15.52	9.815
<i>Partitioned by moneyness</i>				
Delta<0.3	36.55	29.30	25.22	13.58
0.3≤Delta<0.4	31.16	25.64	21.19	11.66
0.4≤Delta<0.5	25.81	22.17	17.05	9.540
0.5≤Delta<0.6	20.56	19.05	12.62	7.145
0.6≤Delta<0.7	18.51	17.39	9.373	6.883
0.7≤Delta	16.81	15.81	8.670	9.381
<i>Partitioned by maturity</i>				
DTM<30	28.51	22.73	16.86	11.92
30≤DTM<60	25.27	21.61	15.64	8.372
60≤DTM<90	20.23	18.80	14.07	7.737
90≤DTM<120	19.73	19.22	14.34	8.809
120≤DTM<150	18.02	17.64	14.11	9.539
150≤DTM	21.33	21.02	15.27	10.62
<i>Partitioned by the level of VIX</i>				
VIX<15	32.40	24.86	17.71	10.82
15≤VIX<20	19.31	18.82	15.62	9.580
20≤VIX<25	14.41	18.11	12.99	8.233
25≤VIX<30	16.27	17.42	13.20	9.281
30≤VIX<35	18.40	17.24	13.32	9.569
35≤VIX	27.69	21.02	12.43	9.924

Note: This table report the out-of-sample option pricing performance for each model. We conduct our out-of-sample performance evaluation by splitting our original dataset into two subsamples: the in-sample data consists of the years before 2008 and the out-of-sample consists of the years 2008-2021, which spans a 14-year period. The estimation for each model is done only once for the in-sample data, and then price the out-of-sample data by the estimated parameters. Therefore, the in-sample data is 1990-2007. We evaluate the model's option pricing ability through the root of mean square errors of log implied volatility. We summarize the results by option moneyness, maturity and market VIX level. Moneyness is measured by Delta computed from the Black-Scholes model. DTM denotes the number of calendar days to maturity. The numbers in shaded region indicate the minimum value within each row in each time period.

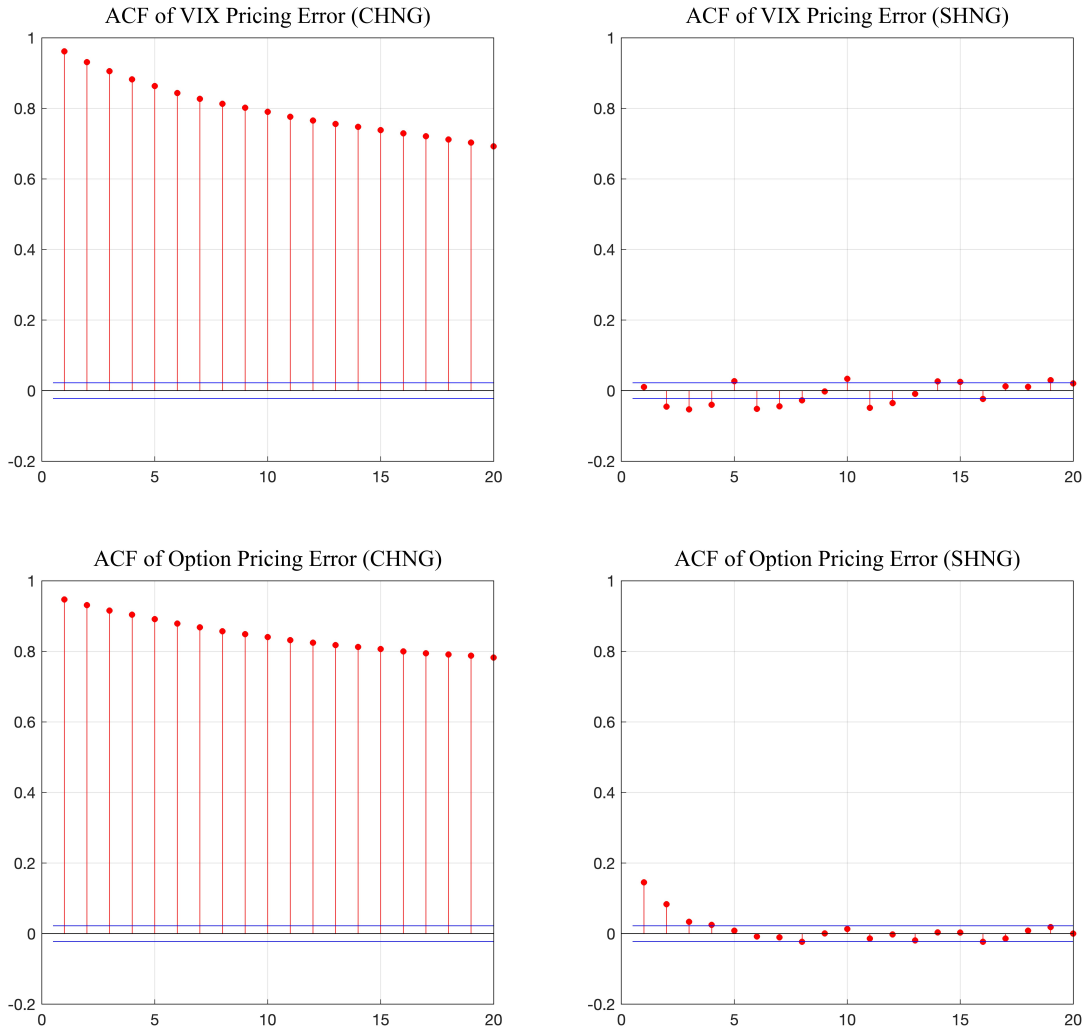


Figure 6: The autocorrelation function (ACF) for derivative pricing errors. The ACFs for the VIX are in the upper panels and the ACFs for the average option pricing error are in the lower panels. Left panels present results for the CHNG model and the right panels for the SHNG model.

prices. While these two specifications have similar point estimates and yield very similar paths for η_t , their differences are large enough to influence derivative pricing. Overall, the out-of-sample results are very encouraging and consistent with the in-sample results.

5.4.1 Insight offered by Autocorrelations

Some key insight about the improvements offered by SHNG specifications can be found in the autocorrelations of pricing errors. The estimated SHNG models show that there is substantial time-variation in η_t . This has important implications for the CHNG model. Because the CHNG model rely on a constant η , the CHNG will have a tendency to make positive pricing errors when η_t is small and negative pricing errors when η_t is large. Moreover, since η_t is found to be highly persistent, we would expect this to induce autocorrelation in the pricing errors. This is indeed what we find empirically, as shown in Figure 6. The upper panels present the autocorrelation functions (ACF) for the VIX pricing errors for CHNG and SHNG estimated with VIX data, and the lower panels present the ACFs for option pricing errors for CHNG and SHNG estimated with option prices. The left panels of Figure 6 show that a constant η induces a high degree of predictability in the pricing errors. This is in stark contrast to the results for the SHNG model in the right panels, where the ACFs are substantially closer to zero. The exception is the first few autocorrelations in the lower-right panels, that are significantly different from zero. The remarkable reduction of these autocorrelations is an excellent illustration of the principle behind score-driven models. In the SHNG model, the variance risk ratio, η_t , is constantly adjusted as dictated by the local first order conditions. This is key to understanding how the SHNG model leads to more accurate derivative pricing. The score-driven approach monitors the first-order conditions and constantly makes adjustment that are proportional to the signal, s_t . As a consequence, the first-order condition is closer to being satisfied throughout the sample, rather than just on average over the full sample period. The large reduction in systematic pricing errors explains the large reducing in the autocorrelations of pricing errors.

5.5 Adaptive Compensation for Misspecification

The adaptive structure of the SHNG model, where parameters are adjusted in the direction dictated by the first-order conditions, makes the resulting derivative pricing formulae robust to model misspecification. The reason is that η_t is automatically adjusted to compensate for misspecification that would otherwise increase pricing errors. While this is a strength of the model structure, it shows that misspecification can undermine the interpretation of η_t as the variance risk ratio.

Expected volatility under \mathbb{Q} is measured with high accuracy, because it can be inferred from observable derivative prices. The situation is different under \mathbb{P} , where we must rely on a model to defines expected volatility. If the model is misspecified, then the model-based expected volatility can be biased. One form of misspecification is parameter instability.

Sichert (2022) showed that a GARCH model with structural breaks can absolve the pricing kernel puzzle relate to the inverted U-shape. This phenomenon is also seen in Tong et al. (2022). They estimate a Markov switching Realized GARCH model with two states, and find the variance risk premium to be positive in both states. The two estimates corresponding to two distinct U -shapes of the pricing kernels, where the quadratic term is close to zero in the low-volatility regime.

If the model-based expected volatility is biased, then this will translate to η_t being biased, in which case η_t need not reflect the true variance risk ratio. For instance, a small value of η_t need not reflect an investor appetite for variance risk, because it could be an artifact of the Heston-Nandi model predicting the future volatility to be higher than true expectations under \mathbb{P} .

As a robustness check, we have computed an alternative variance risk ratio that does not rely on the Heston-Nandi GARCH model. It is based on model-free realized variances and employ a simple AR(1) model to define expected variance under \mathbb{P} . The resulting alternative measure of the variance risk ratio is reported in Appendix B, and its time series is very similar to those for η_t in Figure 5. This shows that the observed fluctuations in η_t is not induced by a flaw that is specific to the GARCH model (1-2). An oversimplified description of expected volatility could be the explanation. The AR(1) model and standard GARCH models entail volatility forecast with mean-reverting features.

We also inspect if the prediction errors in Appendix B in greater details, and their relation to the level of η_t . The errors do not appear to depend on η_t in a systematic.

6 Variance Risk Aversion and Economic Fundamentals

Time variation in the volatility risk aversion is the key characteristic of the new pricing kernel. In this section, we related the time variation in η_t with economic fundamentals and several other variables that are popular in the asset pricing literature.

We focus on seven core measures of uncertainty, disagreement, and sentiment. The first set of variables are related to investor disagreements and we follow Bollerslev et al. (2018) and use two types of proxies for disagreement. The first concerns macroeconomy fundamentals, where we use the forecast dispersion for both unemployment rate and GDP growth in the Survey of Professional Forecasters.¹⁶ The second is disagreement about economic policy, where we adopt the economic policy uncertainty index by Baker et al. (2016). We also include the *variance risk premium* by Carr and Wu (2008), which Grith et al. (2017) argues is a proxy for market uncertainty.¹⁷ We also include three uncertainty measures from existing literature: The *Economic Uncertainty Index* by Bali et al. (2014); the *Survey-based*

¹⁶Bollerslev et al. (2018) only use the forecast dispersion for one-quarter-ahead unemployment rate.

¹⁷Up-to-date VRP series was downloaded from Hao Zhou's website: <https://sites.google.com/site/haozhouspersonalhomepage/>

Uncertainty index by Ozturk and Sheng (2018);¹⁸ and the *Sentiment* variable by Baker and Wurgler (2006). In addition to these seven core variables, we include the economic variables previously used in Baker and Wurgler (2006) and Welch and Goyal (2007), which we label as “control variables”. Most variables are available at a monthly frequency. We will, for this reason, take monthly average of η_t and regress the logarithmically transformed average on the variables listed above (and subsets of these variables).

The regression results are listed in Table 5, where the seven core variables are listed in the top of the table, followed by the six control variables that contributed the most to explaining variation in η_t . There are eleven additional control variables, labelled “Other Controls” which were largely insignificant, and to conserve space the results for these variables are presented in the Web-Appendix.¹⁹ The Web-Appendix also includes various diagnostics to rule out that our estimates are driven by spurious regression results.²⁰

The first column in Table 5 is the specification that only includes the control variables, and these can explain 64.9% of the variation in the monthly average of η . The six most significant control variables are: stock market volatility, the dividend price ratio, and four variables related to interest rates and credit risk.

Columns two to eight present the results for the specification that include a single core variable, in addition to the control variables. Every core variable is significant in these regressions and the signs of their estimated coefficients are consistent with expectation. The sentiment variables is estimated to have a negative coefficient, such that low sentiment is associated with high volatility risk aversion. The following five variables are related to uncertainty, and they all have positive coefficients. So, high uncertainty is associated with high volatility aversion. Finally, the variance risk premium is an empirical measure of the difference between volatility under \mathbb{Q} and \mathbb{P} . It is therefore not surprising that this variables has a positive coefficient and increases the R^2 by the largest amount. The last column is a “kitchen sink regression” that includes all explanatory variables. Most of the variables in Table 5 continue to be significant in this regression and the R^2 increases to nearly 83%. Two of core variables, Forecast Dispersion of GDP Growth and the Economic Uncertainty Index, become insignificant in the kitchen sink regression. This could be due to collinearity, because these two core variables have the largest correlation, (65.7%), of all core variables.

¹⁸This index is constructed from the Consensus Forecasts publication by Consensus Economics Inc. Up-to-date data were downloaded from the website: <https://www.american.edu/cas/faculty/sheng.cfm>

¹⁹We follow Welch and Goyal (2007) in the definitions of these variables. Thus, the yield spread is the difference between BAA- and AAA- rated corporate bond yields, default return spread is the difference between the return on long-term corporate bonds and government bonds, etc. see Welch and Goyal (2007) for details.

²⁰Spurious regression results can arise in a context, such as this one, with highly persistent variables. However, the unit root hypothesis is rejected for all variable in the regression, and the regression residual have little autocorrelation.

Table 5: Economic Explanation for Time-Varying Variance Risk Aversion

	Log Variance Risk Ratio (Monthly Average)				
Sentiment	-0.118*** (0.018)				-0.099*** (0.014)
Dispersion-UNEMP		0.653*** (0.115)			0.254*** (0.095)
Dispersion-GDP			0.236*** (0.065)		0.079 (0.053)
Economic Policy Uncertainty				0.258*** (0.044)	0.203*** (0.035)
Survey-based Uncertainty				0.106*** (0.025)	0.065*** (0.020)
Economic Uncertainty Index				0.037*** (0.008)	-0.007 (0.008)
Variance Risk Premium				0.097*** (0.008)	0.074*** (0.007)
Stock Market Volatility	0.317*** (0.030)	0.318*** (0.028)	0.300*** (0.030)	0.297*** (0.030)	0.202*** (0.026)
Default Yield Spread	0.162*** (0.051)	0.108** (0.048)	0.143*** (0.050)	0.093* (0.052)	0.160*** (0.041)
Default Return Spread	0.031*** (0.007)	0.031*** (0.006)	0.028*** (0.007)	0.029*** (0.007)	0.024*** (0.006)
Long Term Yield	0.040*** (0.009)	0.046*** (0.008)	0.027*** (0.009)	0.056*** (0.009)	0.033*** (0.008)
Dividend Price Ratio	-0.158** (0.070)	-0.158** (0.065)	-0.135* (0.069)	-0.233*** (0.068)	-0.179*** (0.052)
Term Spread	-0.010 (0.010)	-0.021** (0.010)	-0.020** (0.010)	-0.027*** (0.010)	0.004 (0.008)
Other Controls	YES	YES	YES	YES	YES
R^2	0.649	0.693	0.663	0.683	0.770
$\rho(1)$	0.617	0.566	0.611	0.607	0.387

Note: The controlled economic variables are taken from [Welch and Goyal \(2007\)](#) and [Baker and Wurgler \(2006\)](#). Unreported other controls including six macro variables used in [Baker and Wurgler \(2006\)](#) to control the macroeconomic conditions and five variables from [Welch and Goyal \(2007\)](#). The former includes monthly growth rate of industrial production index, real durables consumption, real nondurables consumption, real services consumption, employment and NBER recession indicator. The latter includes earnings price ratio, book to market ratio, net equity expansion, long term rate of return, consumer price index. Most of the results for these unreported other controls are insignificant.

7 Summery

We have introduced a novel approach to derivative pricing by introducing time-varying risk aversion in the pricing kernel. An elegant and tractable framework emerges when the pricing kernel is combined with the Heston-Nandi GARCH model. In this framework, the variance risk ratio is found to be *the* fundamental variable. This variable characterizes all time-variation in the pricing kernel. It is functionally tied to the variance risk aversion parameter that define the curvature of the pricing kernel, and we showed that the framework can generate the shapes of the pricing kernel that are seen empirically. This framework made it possible to derive closed-form expression for the VIX and option prices. In the most general setting where the variance risk aversion is driven by a stochastic process, we derive an option pricing formula that is based on a novel approximation method. The approximation method uses the insight provided by VIX formula, which is valid with predetermined and random variance risk ratio, to determine an adjusted volatility level that yields the correct VIX pricing, when the random variation in the variance risk ratio is neglected. When applied to option prices the resulting approximation works very well. Empirically, we have documented that the proposed framework can greatly reduce derivative pricing errors. The root mean square error of the derivative pricing errors is typically reduced by more than 50% by allowing the variance risk ratio to be time-varying. A reduction of this magnitude was found in-sample as well as out-of-sample. We also found that that our key variable, the variance risk ratio, is closely related to a range of well-known measures of sentiment, disagreement, and uncertainty, as well as key economic variables.

The key idea in this paper is to model time variation in the pricing kernel parameters, where the dynamic properties are driven by suitable first order conditions. In this paper we have applied the idea to the Heston-Nandi GARCH model, but it is also applicable to other models. For instance, it could be used in conjunction with other popular GARCH models, such as EGARCH, GJR-GARCH, and NGARCH, see [Nelson \(1991\)](#), [Glosten et al. \(1993\)](#), and [Engle and Ng \(1993\)](#). The same idea can also be applied to modern volatility models that utilize realized measures of volatility, such as Realized GARCH models by [Hansen et al. \(2012\)](#) and [Hansen and Huang \(2016\)](#), the GARV model by [Christoffersen et al. \(2014\)](#), and the LHARG, see [Majewski et al. \(2015\)](#). Closed-form option pricing formula will likely be unattainable once time-varying variance risk aversion is introduced to these model. However approximation methods, such as those by [Duan et al. \(1999\)](#), may be used instead.

In this paper, we have introduced time-variation to the pricing kernel, while maintaining the model with constant parameters under \mathbb{P} . So, the time-variation that is introduced in the pricing kernel get parsed to the model under \mathbb{Q} . While this induces time variation in ξ that governs the variance risk premium, the equity risk parameter, λ , is constant, because it defined by the model under \mathbb{P} . The score-driven approach could be used to introduce time-variation in λ (and other parameters) but would require a more flexible (and time-varying)

model under \mathbb{P} . We leave this for future work.

References

- Aït-Sahalia, Y. and Lo, A. W. (2000). Nonparametric risk management and implied risk aversion. *Journal of Econometrics*, 94:9–51.
- Andersen, T. G., Bollerslev, T., Diebold, F. X., and Labys, P. (2003). Modeling and Forecasting Realized Volatility. *Econometrica*, 71(2):579–625.
- Andries, M., Eisenbach, T. M., and Schmalz, M. C. (2018). Horizon-dependent risk aversion and the timing and pricing of uncertainty. *FRB of New York Staff Report*, (703).
- Arrow, K. J. and Debreu, G. (1954). Existence of an equilibrium for a competitive economy. *Econometrica*, 22:265–290.
- Baker, M. and Wurgler, J. (2006). Investor sentiment and the cross-section of stock returns. *The journal of Finance*, 61:1645–1680.
- Baker, S. R., Bloom, N., and Davis, S. J. (2016). Measuring economic policy uncertainty. *The quarterly journal of economics*, 131:1593–1636.
- Bakshi, G., Cao, C., and Chen, Z. (1997). Empirical performance of alternative option pricing models. *The Journal of Finance*, 52:2003–2049.
- Bakshi, G. and Madan, D. (2008). Investor heterogeneity and the non-monotonicity of the aggregate marginal rate of substitution in the market index. *Unpublished working paper, University of Maryland*.
- Bakshi, G., Madan, D., and Panayotov, G. (2010). Returns of claims on the upside and the viability of u-shaped pricing kernels. *Journal of Financial Economics*, 97:130–154.
- Bali, T. G., Brown, S. J., and Caglayan, M. O. (2014). Macroeconomic risk and hedge fund returns. *Journal of Financial Economics*, 114:1–19.
- Bali, T. G. and Zhou, H. (2016). Risk, uncertainty, and expected returns. *Journal of Financial and Quantitative Analysis*, 51:707–735.
- Barone-Adesi, G., Engle, R. F., and Mancini, L. (2008). A GARCH option pricing model with filtered historical simulation. *Review of Financial Studies*, 21:1223–1258.
- Beare, B. K. and Schmidt, L. D. (2016). An empirical test of pricing kernel monotonicity. *Journal of Applied Econometrics*, 31:338–356.
- Bekaert, G., Engstrom, E. C., and Xu, N. R. (2020). The time variation in risk appetite and uncertainty. *NBER*.

- Blasques, F., Koopman, S. J., and Lucas, A. (2015). Information-theoretic optimality of observation-driven time series models for continuous responses. *Biometrika*, 102:325–343.
- Bollerslev, T. (1986). Generalized autoregressive heteroskedasticity. *Journal of Econometrics*, 31:307–327.
- Bollerslev, T., Gibson, M., and Zhou, H. (2011). Dynamic estimation of volatility risk premia and investor risk aversion from option-implied and realized volatilities. *Journal of Econometrics*, 160:235–245.
- Bollerslev, T., Li, J., and Xue, Y. (2018). Volume, volatility, and public news announcements. *The Review of Economic Studies*, 85:2005–2041.
- Bollerslev, T., Tauchen, G., and Zhou, H. (2009). Expected Stock Returns and Variance Risk Premia. *The Review of Financial Studies*, 22:4463–4492.
- Broadie, M., Chernov, M., and Johannes, M. (2007). Model specification and risk premia: Evidence from futures options. *The Journal of Finance*, 62:1453–1490.
- Brown, D. P. and Jackwerth, J. C. (2012). The pricing kernel puzzle: Reconciling index option data and economic theory. In *Derivative Securities Pricing and Modelling*, pages 155–183. Emerald Group Publishing Limited.
- Campbell, J. Y. and Cochrane, J. H. (1999). By force of habit: A consumption-based explanation of aggregate stock market behavior. *Journal of political Economy*, 107:205–251.
- Carr, P. and Wu, L. (2008). Variance Risk Premiums. *The Review of Financial Studies*, 22:1311–1341.
- Chabi-Yo, F. (2012). Pricing kernels with stochastic skewness and volatility risk. *Management Science*, 58:624–640.
- Chabi-Yo, F., Garcia, R., and Renault, E. (2008). State dependence can explain the risk aversion puzzle. *Review of Financial Studies*, 21:973–1011.
- Chabi-Yo, F. and Song, Z. (2013). Recovering the probability weights of tail events with volatility risk from option prices. Technical report, Working Paper, Ohio State University.
- Chen, X. and Ghysels, E. (2011). News – good or bad – and its impact on volatility predictions over multiple horizons. *Review of Financial Studies*, 24:46–81.
- Chernov, M. and Ghysels, E. (2000). A study towards a unified approach to the joint estimation of objective and risk neutral measures for the purpose of options valuation. *Journal of Financial Economics*, 56:407–458.

- Christoffersen, P., Feunou, B., Jacobs, K., and Meddahi, N. (2014). The economic value of realized volatility: Using high-frequency returns for option valuation. *Journal of Financial and Quantitative Analysis*, 49:663–697.
- Christoffersen, P., Heston, S. L., and Jacobs, K. (2013). Capturing option anomalies with a variance-dependent pricing kernel. *Review of Financial Studies*, 26:1963–2006.
- Corsi, F., Fusari, N., and Vecchia, D. L. (2013). Realizing smiles: Options pricing with realized volatility. *Journal of Financial Economics*, 107:284–304.
- Cox, J. C., Ingersoll, J. E., and Ross, S. A. (1985). A theory of the term structure of interest rates. *Econometrica*, 53:385–408.
- Creal, D. D., Koopman, S. J., and Lucas, A. (2013). Generalized autoregressive score models with applications. *Journal of Applied Econometrics*, 28:777–795.
- Cuesdeanu, H. and Jackwerth, J. C. (2018). The pricing kernel puzzle in forward looking data. *Review of Derivatives Research*, 21:253–276.
- Duan, J.-C. (1995). The GARCH option pricing model. *Mathematical finance*, 5:13–32.
- Duan, J.-C., Gauthier, G., and Simonato, J. (1999). An analytical approximation for the GARCH option pricing model. *Journal of Computational Finance*, 2:75–116.
- Eisenbach, T. M. and Schmalz, M. C. (2016). Anxiety in the face of risk. *Journal of Financial Economics*, 121:414–426.
- Engle, R. F. (1982). Autoregressive conditional heteroskedasticity with estimates of the variance of U.K. inflation. *Econometrica*, 45:987–1007.
- Engle, R. F. and Ng, V. K. (1993). Measuring and Testing the Impact of News on Volatility. *Journal of Finance*, 48:1749–78.
- Feller, W. (1951). Two singular diffusion problems. *Annals of mathematics*, pages 173–182.
- Feunou, B. and Okou, C. (2019). Good volatility, bad volatility, and option pricing. *Journal of Financial and Quantitative Analysis*, 54:695–727.
- Glosten, L. R., Jagannathan, R., and Runkle, D. E. (1993). On the Relation between the Expected Value and the Volatility of the Nominal Excess Return on Stocks. *Journal of Finance*, 48:1779–1801.
- González, M., Nave, J., and Rubio, G. (2018). Macroeconomic determinants of stock market betas. *Journal of Empirical Finance*, 45:26–44.
- Grith, M., Härdle, W. K., and Krätschmer, V. (2017). Reference-dependent preferences and the empirical pricing kernel puzzle. *Review of Finance*, 21:269–298.

- Han, B. (2008). Investor sentiment and option prices. *The Review of Financial Studies*, 21:387–414.
- Hansen, P. R. and Huang, Z. (2016). Exponential GARCH modeling with realized measures of volatility. *Journal of Business & Economic Statistics*, 34:269–287.
- Hansen, P. R., Huang, Z., and Shek, H. (2012). Realized GARCH: A joint model of returns and realized measures of volatility. *Journal of Applied Econometrics*, 27:877–906.
- Hao, J. and Zhang, J. E. (2013). GARCH option pricing models, the CBOE VIX, and variance risk premium. *Journal of Financial Econometrics*, 11:556–580.
- Heston, S. L. (1993). A closed-form solution for options with stochastic volatility with applications to bond and currency options. *Review of Financial Studies*, 6:327–343.
- Heston, S. L. and Nandi, S. (2000). A closed-form GARCH option valuation model. *Review of Financial Studies*, 13:585–625.
- Huang, Z., Wang, T., and Hansen, P. R. (2017). Option pricing with the realized GARCH model: An analytical approximation approach. *Journal of Futures Markets*, 37:328–358.
- Jackwerth, J. C. (2000). Recovering risk aversion from option prices and realized returns. *The Review of Financial Studies*, 13:433–451.
- Kiesel, R. and Rahe, F. (2017). Option pricing under time-varying risk-aversion with applications to risk forecasting. *Journal of Banking & Finance*, 76:120–138.
- Koopman, S. J., Lucas, A., and Scharth, M. (2016). Predicting time-varying parameters with parameter-driven and observation-driven models. *Review of Economics and Statistics*, 98:97–110.
- Li, G. (2007). Time-varying risk aversion and asset prices. *Journal of Banking & Finance*, 31:243–257.
- Lucas, R. E. (1978). Asset prices in an exchange economy. *Econometrica*, 46:1429–1445.
- Majewski, A. A., Bormetti, G., and Corsi, F. (2015). Smile from the past: A general option pricing framework with multiple volatility and leverage components. *Journal of Econometrics*, 187:521–531.
- Nelson, D. B. (1991). Conditional heteroskedasticity in asset returns: A new approach. *Econometrica*, 59:347–370.
- Ornthanalai, C. (2014). Levy jump risk: Evidence from options and returns. *Journal of Financial Economics*, 112(1):69–90.

- Ozturk, E. O. and Sheng, X. S. (2018). Measuring global and country-specific uncertainty. *Journal of International Money and Finance*, 88:276–295.
- Polkovnichenko, V. and Zhao, F. (2013). Probability weighting functions implied in options prices. *Journal of Financial Economics*, 107:580–609.
- Rosenberg, J. V. and Engle, R. F. (2002). Empirical pricing kernels. *Journal of Financial Economics*, 64:341–372.
- Rubinstein, M. (1976). The valuation of uncertain income streams and the pricing of options. *Bell Journal of Economics*, 7:407–425.
- Shefrin, H. (2001). On kernels and sentiment. *Available at SSRN 288258*.
- Shefrin, H. (2008). Risk and return in behavioral SDF-based asset pricing models. *Journal of Investment Management*, 6:1–18.
- Sichert, T. (2022). The pricing kernel is U-shaped. *Working Paper*.
- Song, Z. and Xiu, D. (2016). A tale of two option markets: Pricing kernels and volatility risk. *Journal of Econometrics*, 190:176–196.
- Tong, C., Hansen, P. R., and Huang, Z. (2022). Option pricing with state-dependent pricing kernel. *Journal of Futures Prices*, 42:1409–1433.
- Wang, T., Shen, Y., Jiang, Y., and Huang, Z. (2017). Pricing the CBOE VIX futures with the Heston–Nandi GARCH model. *Journal of Futures Markets*, 37(7):641–659.
- Welch, I. and Goyal, A. (2007). A comprehensive look at the empirical performance of equity premium prediction. *The Review of Financial Studies*, 21:1455–1508.

A Appendix of Proofs

A.1 Proof of Theorem 1

The pricing kernel with dynamic risk parameters takes the form

$$M_{t+1,t} = \frac{\exp(\phi_t R_{t+1} + \xi_t h_{t+2})}{\mathbb{E}_t^{\mathbb{P}}[\exp(\phi_t R_{t+1} + \xi_t h_{t+2})]},$$

where the parameters ϕ_t and ξ_t are \mathcal{G}_t -measurable. The pricing kernel implies some dynamic properties in risk neutral measure satisfying the no-arbitrage conditions: $\mathbb{E}_t^{\mathbb{P}}[M_{t+1,t}] = 1$ and $\mathbb{E}_t^{\mathbb{P}}[M_{t+1,t} \exp(R_{t+1})] = \exp(r)$. The first is trivial, whereas the second condition reads

$$\frac{\mathbb{E}_t^{\mathbb{P}}[\exp\{(\phi_t + 1)R_{t+1} + \xi_t h_{t+2}\}]}{\mathbb{E}_t^{\mathbb{P}}[\exp(\phi_t R_{t+1} + \xi_t h_{t+2})]} = \exp(r). \quad (\text{A.1})$$

The moments generating function of (R_{t+1}, h_{t+2}) under \mathbb{P} is

$$\begin{aligned} \mathbb{E}_t^{\mathbb{P}}[\exp(v_1 R_{t+1} + v_2 h_{t+2})] &= \exp\left[v_1 r + v_2 \omega + [v_1(\lambda - \frac{1}{2}) + v_2(\beta + \alpha\gamma^2)]h_{t+1}\right] \\ &\quad \times \mathbb{E}_t^{\mathbb{P}}\left[v_2 \alpha z_{t+1}^2 + (v_1 - 2v_2 \alpha \gamma) \sqrt{h_{t+1}} z_{t+1}\right] \\ &= \exp\left[v_1 r + v_2 \omega + [v_1(\lambda - \frac{1}{2}) + v_2(\beta + \alpha\gamma^2)]h_{t+1}\right. \\ &\quad \left. - \frac{1}{2} \log(1 - 2v_2 \alpha) + \frac{(v_1 - 2v_2 \alpha \gamma)^2}{2(1 - 2v_2 \alpha)} h_{t+1}\right] \\ &= \exp\left[v_1 r + v_2 \omega - \frac{1}{2} \log(1 - 2v_2 \alpha)\right. \\ &\quad \left. + \left(v_1(\lambda - \frac{1}{2}) + v_2(\beta + \alpha\gamma^2) + \frac{(v_1 - 2v_2 \alpha \gamma)^2}{2(1 - 2v_2 \alpha)}\right) h_{t+1}\right]. \end{aligned}$$

Substituting $(\phi_{t+1} + 1, \xi_t)$ and (ϕ_{t+1}, ξ_t) for (v_1, v_2) and taking their ratio, reveals that (A.1) simplifies to $[\lambda - \frac{1}{2} + \frac{1 + 2\phi_t - 4\xi_t \alpha \gamma}{2(1 - 2\xi_t \alpha)}]h_{t+1} = 0$. Next, solving for λ yields

$$\lambda = \eta_t \left(\gamma - \phi_t - \frac{1}{2}\right) - \gamma + \frac{1}{2}, \quad \text{where } \eta_t \equiv \frac{1}{1 - 2\alpha\xi_t}, \quad (\text{A.2})$$

and the results stated in part (i) of Theorem 1 are established.

The risk-neutral dynamic is deduced from the moments generating function of z_{t+1} under the \mathbb{Q} measure is:

$$\begin{aligned} \mathbb{E}_t^{\mathbb{Q}}[\exp(v_1 z_{t+1})] &= \exp\left[\left(\frac{\phi_t - 2\xi_t \alpha \gamma}{1 - 2\xi_t \alpha} \sqrt{h_{t+1}}\right) v_1 + \frac{1}{2(1 - 2\xi_t \alpha)} v_1^2\right] \\ &= \exp\left[\left[-\left(\lambda + \frac{1}{2}\eta_t - \frac{1}{2}\right) \sqrt{h_{t+1}}\right] v_1 + \frac{1}{2}\eta_t v_1^2\right] \end{aligned} \quad (\text{A.3})$$

The last equality comes from (A.2). The expression (A.3) shows that z_{t+1} is also normally distributed under \mathbb{Q} , but with a different mean and a different variance (than under \mathbb{P}). So

we define

$$z_{t+1}^* = \frac{z_{t+1} - \mathbb{E}_t^{\mathbb{Q}}(z_{t+1})}{\sqrt{\text{var}^{\mathbb{Q}}(z_{t+1})}} = \frac{1}{\sqrt{\eta_t}} \left(z_{t+1} + \left(\lambda + \frac{1}{2}\eta_t - \frac{1}{2} \right) \sqrt{h_{t+1}} \right), \quad t = 1, 2, \dots, \quad (\text{A.4})$$

such that $z_t^* \sim iidN(0, 1)$ under \mathbb{Q} . Substituting the risk-neutralized quantities, z_{t+1}^* and $h_{t+1}^* = \eta_t h_{t+1}$ into (1), we arrive at the expressions stated in part (ii). Finally, part (iii) is an implication of the MGF for z_{t+1} under \mathbb{Q} , see (A.3). \square

A.2 Proof of Theorem 2

We rewrite the volatility dynamic under \mathbb{Q} measure as

$$h_{t+1}^* = (\omega_t^* + \alpha_t^*) + (\beta_t^* + \alpha_t^* \gamma_{t-1}^{*2}) h_t^* + \nu_t,$$

where $\nu_t = \alpha_t^* ((z_t^*)^2 - 1 - 2\gamma_{t-1}^* z_t^* \sqrt{h_t^*})$ is a zero-mean variation condition on \mathcal{F}_{t-1} . We denote $A_t \equiv \omega_t + \alpha_t$ and $B_t \equiv \beta_t^* + \alpha_t \gamma_{t-1}^{*2}$, then we have

$$\begin{aligned} h_{t+k}^* &= A_{t+k-1} + B_{t+k-1} h_{t+k-1}^* + \nu_{t+k-1} \\ &= A_{t+k-1} + B_{t+k-1} A_{t+k-2} + B_{t+k-1} B_{t+k-2} h_{t+k-2}^* + B_{t+k-2} \nu_{t+k-2} + \nu_{t+k-1} \\ &= A_{t+k-1} + B_{t+k-1} A_{t+k-2} + \dots + B_{t+k-1} \dots B_{t+2} A_{t+1} + B_{t+k-1} \dots B_{t+1} h_{t+1}^* \\ &\quad + \sum_{i=1}^{t+k-1} B_{t+k-2} \dots B_i \nu_i. \end{aligned}$$

In order to get its analytical formula, we replace B_t with $\tilde{B}_t \equiv \beta_t^* + \alpha_t \tilde{\gamma}_{t-1}^{*2}$ where $\tilde{\gamma}_t^* = \frac{1}{\eta_t}(\gamma + \lambda)$. Empirically $\tilde{\gamma}_t^*$ is indistinguishable from $\gamma_t^* = \frac{1}{\eta_t}(\gamma + \lambda + \frac{1}{2}(\eta_t - 1))$ because the magnitude of $\gamma + \lambda$ is much larger than $\frac{1}{2}(\eta_t - 1)$. Empirically we have $\gamma + \lambda \approx 280$ whereas $\frac{1}{2}(\eta_t - 1)$ ranges between -0.25 and 1.5 , with an average value of about 0.1 .

It follows that²¹

$$\tilde{B}_t = \beta_t^* + \alpha_t^* \gamma_{t-1}^{*2} = \beta \frac{\eta_t}{\eta_{t-1}} + \alpha \eta_t \eta_{t-1} \left(\frac{\gamma + \lambda}{\eta_{t-1}} \right)^2 = \tilde{\beta} \frac{\eta_t}{\eta_{t-1}},$$

where $\tilde{\beta} \equiv \beta + \alpha(\gamma + \lambda)^2$, so that $\tilde{B}_{t+k} \tilde{B}_{t+k-1} \dots \tilde{B}_{t+i} = \tilde{\beta}^{k-i+1} \frac{\eta_{t+k}}{\eta_{t+i-1}}$, and

$$\tilde{B}_{t+k} \dots \tilde{B}_{t+i+1} A_{t+i} = \tilde{\beta}^{k-i} \frac{\eta_{t+k}}{\eta_{t+i}} (\omega \eta_{t+i} + \alpha \eta_{t+i} \eta_{t+i-1}) = \tilde{\beta}^{k-i} (\omega \eta_{t+k} + \alpha \eta_{t+k} \eta_{t+i-1}).$$

²¹Recall that $\alpha_t^* = \alpha \eta_t \eta_{t-1}$ and $\beta_t^* = \beta \frac{\eta_t}{\eta_{t-1}}$.

Using these results, we have

$$\mathbb{E}_t^{\mathbb{Q}}(h_{t+k}^*) = \sum_{i=2}^k \tilde{\beta}^{k-i} \mathbb{E}_t^{\mathbb{Q}}(\omega \eta_{t+k-1} + \alpha \eta_{t+k-1} \eta_{t+i-2}) + \tilde{\beta}^{k-1} \mathbb{E}_t^{\mathbb{Q}}\left(\frac{\eta_{t+k-1}}{\eta_t}\right) h_{t+1}^* + \delta_k,$$

where δ_k is the term that arises from the substitution of \tilde{B}_t for B_t .

The M -days ahead VIX can be calculated as the annualized arithmetic average of the expected daily variance over the following month under the risk-neutral measure, i.e.

$$\text{VIX}_t = A \times \sqrt{\frac{1}{M} \sum_{k=1}^M \mathbb{E}_t^{\mathbb{Q}}(h_{t+k}^*)}.$$

Where $A = 100\sqrt{252}$ is the annualizing factor. The model-implied squared VIX is given by,

$$\begin{aligned} \frac{A^2}{M} \sum_{k=1}^M \mathbb{E}_t^{\mathbb{Q}}(h_{t+k}^*) &= \underbrace{\frac{A^2}{M} \sum_{k=2}^M \sum_{i=2}^k \tilde{\beta}^{k-i} \mathbb{E}_t^{\mathbb{Q}}(\omega \eta_{t+k-1} + \alpha \eta_{t+k-1} \eta_{t+i-2})}_{a_1(\eta_t, M, \sigma^2)} \\ &\quad + \underbrace{\frac{A^2}{M} \sum_{k=1}^M \tilde{\beta}^{k-1} \mathbb{E}_t^{\mathbb{Q}}\left(\frac{\eta_{t+k-1}}{\eta_t}\right) h_{t+1}^*}_{a_2(\eta_t, M, \sigma^2)} + \Delta, \end{aligned} \quad (\text{A.5})$$

where $\Delta = \frac{A^2}{M} \sum \delta_k$. We provide bounds for the approximation error term Δ in Lemma A.1, and show that this term is negligible in practice.

From the AR(1) structure, $\log \eta_t = (1 - \theta)\zeta + \theta \log \eta_{t-1} + \varepsilon_t$, with $|\theta| < 1$, it follows that $\mathbb{E}(\log \eta_t) = \zeta$ and

$$\log \eta_{t+k} = (1 - \theta^k) \zeta + \theta^k \log \eta_t + \sum_{j=0}^{k-1} \theta^j \varepsilon_{t+k-j}.$$

Such that for $i < k$, we have

$$\log(\eta_{t+k} \eta_{t+i}) = (2 - \theta^k - \theta^i) \zeta + (\theta^k + \theta^i) \log \eta_t + \sum_{j=0}^{i-1} 2\theta^j \varepsilon_{t+k-j} + \sum_{j=i}^{k-1} \theta^j \varepsilon_{t+k-j}.$$

Suppose that ε_t is i.i.d and let $\Psi(\phi) \equiv \log \mathbb{E}[\exp(\phi \varepsilon_t)]$ denote its log-MGF. Then we have

$$\mathbb{E}_t(\eta_{t+k}) = \exp\{(1 - \theta^k)\zeta + \theta^k \log \eta_t + \sum_{j=0}^{k-1} \Psi(\theta^j)\},$$

and

$$\mathbb{E}_t(\eta_{t+k} \eta_{t+i}) = \exp\{(2 - \theta^k - \theta^i)\zeta + (\theta^k + \theta^i) \log \eta_t + \sum_{j=0}^{i-1} \Psi(2\theta^j) + \sum_{j=i}^{k-1} \Psi(\theta^j)\}.$$

We can now express the two key terms in (A.5) as,

$$a_1(\eta_t, M, \sigma^2) = \frac{A^2}{M} \sum_{k=2}^M \sum_{i=2}^k \tilde{\beta}^{k-i} \left[\omega \Lambda_1(k) \eta_t^{\theta^{k-1}} + \alpha \Lambda_2(k, i) \eta_t^{\theta^{k-1} + \theta^{i-2}} \right],$$

and

$$a_2(\eta_t, M, \sigma^2) = \frac{A^2}{M} \sum_{k=1}^M \tilde{\beta}^{k-1} \Lambda_1(k) \eta_t^{\theta^{k-1}-1},$$

respectively, where

$$\Lambda_1(k) = \exp \left\{ \left(1 - \theta^{k-1} \right) \zeta + \sum_{j=0}^{k-2} \Psi(\theta^j) \right\},$$

$$\Lambda_2(k, i) = \exp \left\{ \left(2 - \theta^{k-1} - \theta^{i-2} \right) \zeta + \sum_{j=0}^{i-3} \Psi(2\theta^j) + \sum_{j=i-2}^{k-2} \Psi(\theta^j) \right\}.$$

Under the additional assumption that ε_t is normally distributed with variance σ^2 , the two expression simplify to

$$\Lambda_1(k) = \exp \left\{ \left(1 - \theta^{k-1} \right) \zeta + \frac{\sigma^2}{2} \frac{1 - \theta^{2k-2}}{1 - \theta^2} \right\},$$

and

$$\Lambda_2(k, i) = \exp \left\{ \left(2 - \theta^{k-1} - \theta^{i-2} \right) \zeta + 2\sigma^2 \frac{1 - \theta^{2i-4}}{1 - \theta^2} + \frac{\sigma^2}{2} \frac{\theta^{2i-4} - \theta^{2k-2}}{1 - \theta^2} \right\},$$

respectively. □

Lemma A.1 (Bound for Δ). *Suppose that $\eta_t \in [\eta_L, \eta_H]$ is bounded where $\eta_L, \eta_H > 0$. Then $\Delta \leq \delta(\tilde{\beta}_{\max}) - \delta(\tilde{\beta}_{\min})$, where*

$$\delta(x) = A \times \sqrt{\frac{1}{M} \left[\sum_{k=2}^M \sum_{i=2}^k x^{k-i} \mathbb{E}_t^{\mathbb{Q}}(\omega \eta_{t+k-1} + \alpha \eta_{t+k-1} \eta_{t+i-2}) + \sum_{k=1}^M x^{k-1} \mathbb{E}_t^{\mathbb{Q}} \left(\frac{\eta_{t+k-1}}{\eta_t} \right) h_{t+1}^* \right]},$$

and $\tilde{\beta}_{\min} = \beta + \alpha(\gamma + \lambda + \frac{1}{2}(\eta_L - 1))^2$ and $\tilde{\beta}_{\max} = \beta + \alpha(\gamma + \lambda + \frac{1}{2}(\eta_H - 1))^2$.

Proof. We have $B_t = \beta_t^* + \alpha_t^* \gamma_{t-1}^{*2} \in [\tilde{\beta}_{\min}, \tilde{\beta}_{\max}] \frac{\eta_t}{\eta_{t-1}}$. Since $\delta(x)$ is a monotone function in x , there exists an $\tilde{\beta} \in [\tilde{\beta}_{\min}, \tilde{\beta}_{\max}]$, such that $\delta(\tilde{\beta}) = A \times \sqrt{\frac{1}{M} \sum_{k=1}^M \mathbb{E}_t^{\mathbb{Q}}(h_{t+k}^*)}$ (i.e. true value of VIX), and $\Delta^{\text{vix}} = |\delta(\tilde{\beta}) - \delta(\tilde{\beta})|$, then we have $\Delta \leq \delta(\tilde{\beta}_{\max}) - \delta(\tilde{\beta}_{\min})$. Note that $\delta(x)$ can be expressed in terms of $a_1(\eta_t, M, \sigma^2)$ and $a_2(\eta_t, M, \sigma^2)$. □

A.3 Proof of Theorem 3

From [Heston and Nandi \(2000\)](#) we have the analytical formula for the price of an European call option. The remaining problem is to derive the appropriate moment generating function for cumulative returns, for the case where η_t is predetermined, but need not be constant. The appropriate MGF is denoted $g_{t,T}^*(s)$ in the following Lemma [A.2](#).

Lemma A.2. *In the predetermined case, $\eta_\tau = \mathbb{E}_t^{\mathbb{Q}}[\eta_\tau]$ for $\tau = t + 1, \dots, T$. The moments generating function for cumulative returns has the exponentially affine form:*

$$g_{t,T}^*(s) = \mathbb{E}_t^{\mathbb{Q}}(\exp(s \sum_{\tau=t+1}^T R_\tau)) = \exp(A_T(s, M) + \mathcal{B}_T(s, M)h_{t+1}^*),$$

where $\mathcal{A}_T(s, m)$ and $\mathcal{B}_T(s, m)$ are recursively given by

$$\mathcal{A}_T(s, m+1) = \mathcal{A}_T(s, m) + sr + \mathcal{B}_T(m, s)\omega_{T-m}^* - \frac{1}{2} \log(1 - 2\alpha_{T-m}^* \mathcal{B}_T(m, s)), \quad (\text{A.6})$$

$$\mathcal{B}_T(s, m+1) = s(\gamma_{T-m-1}^* - \frac{1}{2}) - \frac{1}{2}\gamma_{T-m-1}^{*2} + \beta_{T-m}^* \mathcal{B}_T(s, m) + \frac{(s - \gamma_{T-m-1}^*)^2}{2(1 - 2\alpha_{T-m}^* \mathcal{B}_T(s, m))}, \quad (\text{A.7})$$

with initial values $\mathcal{A}_T(s, 1) = sr$ and $\mathcal{B}_T(s, 1) = \frac{1}{2}(s^2 - s)$, where all terms in [\(A.6\)](#) and [\(A.7\)](#) are predetermined.

Proof. For later use, we note that the MGF for (R_{t+1}, h_{t+2}^*) is given by:

$$\begin{aligned} \mathbb{E}_t^{\mathbb{Q}}(\exp(sR_{t+1} + uh_{t+2}^*)) &= \exp \left[sr + u\omega_{t+1}^* - \frac{1}{2} \log(1 - 2u\alpha_{t+1}^*) \right. \\ &\quad \left. + \left(s(\gamma_t^* - \frac{1}{2}) + u\beta_{t+1}^* - \frac{1}{2}\gamma_t^{*2} + \frac{(s - \gamma_t^*)^2}{2(1 - 2u\alpha_{t+1}^*)} \right) h_{t+1}^* \right] \end{aligned} \quad (\text{A.8})$$

where we used [Theorem 1](#). Next, we will establish the exponentially affine form,

$$\mathbb{E}_t^{\mathbb{Q}}(\exp(s \sum_{\tau=t+1}^T R_\tau)) = \exp(A_T(s, M) + \mathcal{B}_T(s, M)h_{t+1}^*)$$

where $M = T - t$. This is proven by backwards induction. First we observe that for $t = T - 1$ we have

$$\mathbb{E}_{T-1}^{\mathbb{Q}}(\exp(sR_T)) = \exp[sr + \frac{1}{2}(s^2 - s)h_T^*].$$

So $\mathcal{A}_T(s, 1) = sr$ and $\mathcal{B}_T(s, 1) = \frac{1}{2}(s^2 - s)$ define the initial values for \mathcal{A}_T and \mathcal{B}_T . Next, we establish the recursions for \mathcal{A}_T and \mathcal{B}_T , by showing that the exponentially affine form

holds for $t = T - m$, whenever it holds for $t = T - (m - 1)$. Thus, consider

$$\begin{aligned}
\mathbb{E}_{T-m}^{\mathbb{Q}} \left[\exp \left(s \sum_{\tau=T-m+1}^T R_{\tau} \right) \right] &= \mathbb{E}_{T-m}^{\mathbb{Q}} \left[\exp \left(sR_{T-m+1} + s \sum_{\tau=T-m+2}^T R_{\tau} \right) \right] \\
&= \mathbb{E}_{T-m}^{\mathbb{Q}} \left[\mathbb{E}_{T-m+1}^{\mathbb{Q}} \left[\exp \left(sR_{T-m+1} + s \sum_{\tau=T-m+2}^T R_{\tau} \right) \right] \right] \\
&= \mathbb{E}_{T-m}^{\mathbb{Q}} \left[\exp (sR_{T-m+1}) \mathbb{E}_{T-m+1}^{\mathbb{Q}} \left(s \sum_{\tau=T-m+2}^T R_{\tau} \right) \right] \\
&= \mathbb{E}_{T-m}^{\mathbb{Q}} [\exp (sR_{T-m+1} + A_T(s, m - 1) + B_T(s, m - 1)h_{T-m+2}^*)].
\end{aligned}$$

Now substitute $B_T(s, m - 1)$ for u in (A.8) with $t = T - m$. The exponentially affine form now follows if we set

$$A_T(s, m) = A_T(s, m - 1) + sr + B_T(s, m - 1)\omega_{T-m+1}^* - \frac{1}{2} \log(1 - 2\alpha_{T-m+1}^* B_T(s, m - 1)),$$

and

$$B_T(s, m) = s(\gamma_{T-m}^* - \frac{1}{2}) - \frac{1}{2}\gamma_{T-m}^{*2} + \beta_{T-m+1}^* B_T(s, m - 1) + \frac{(s - \gamma_{T-m}^*)^2}{2(1 - 2\alpha_{T-m+1}^* B_T(s, m - 1))}.$$

There are some interesting differences between the new expressions and the original expressions. Our expressions for $A_T(s, m)$ and $B_T(s, m)$ depend s (the argument of the MGF) and m (days to maturity m), but unlike the original expressions it also depends on T (the maturity date). The reason is that the coefficients, ω^* , α^* , β^* , and γ^* , are time-varying under \mathbb{Q} due to their relation to η_t . \square

A.4 Proof of Therm 5

We observe N_t derivative prices at time t , resulting in the vector of pricing error, $e_t \in \mathbb{R}^{N_t}$. So, the derivative with respect to $\log \eta_t$ is

$$\begin{aligned}
\nabla_t &\equiv \frac{\partial \ell(X_t | \mathcal{G}_t)}{\partial \log \eta_t} = -\frac{1}{2\sigma_e^2} \frac{\partial (e_t' \Omega_{N_t}^{-1} e_t)}{\partial \log \eta_t} \\
&= -\frac{1}{2\sigma_e^2} \frac{\partial (e_t' \Omega_{N_t}^{-1} e_t)}{\partial e_t'} \frac{\partial e_t}{\partial \log \eta_t} \\
&= -\frac{1}{\sigma_e^2} e_t' \Omega_{N_t}^{-1} \frac{\partial e_t}{\partial \log \eta_t} \\
&= \frac{1}{\sigma_e^2} \left(\frac{\partial X_t^m}{\partial \log \eta_t} \right)' \Omega_{N_t}^{-1} e_t,
\end{aligned}$$

such that

$$\mathbb{E}^{\mathbb{P}}[\nabla_t^2 | \mathcal{G}_t] = \frac{1}{\sigma_e^2} \left(\frac{\partial X_t^m}{\partial \log \eta_t} \right)' \Omega_{N_t}^{-1} \left(\frac{\partial X_t^m}{\partial \log \eta_t} \right).$$

In the special case with a single derivative price, $N_t = 1$, our expressions simplify to

$$\nabla_t = \frac{1}{\sigma_e^2} (X_t - X_t^m) \frac{\partial X_t^m}{\partial \log \eta_t} \quad \text{and} \quad \mathbb{E}^{\mathbb{P}}[\nabla_t^2 | \mathcal{G}_t] = \frac{1}{\sigma_e^2} \left(\frac{\partial X_t^m}{\partial \log \eta_t} \right)^2,$$

such that

$$s_t = \frac{1}{\sigma_e} (X_t - X_t^m) \text{sign} \left(\frac{\partial X_t^m}{\partial \log \eta_t} \right).$$

A.4.1 The Distribution of the Score

Define

$$\psi_t' = \frac{1}{\sigma_e^2} \left(\frac{\partial X_t^m}{\partial \log \eta_t} \right)' \Omega_{N_t}^{-1}, \quad \Sigma_{N_t} = \sigma_e^2 \Omega_{N_t}$$

Then the MGF of score s_t can be expressed as

$$\mathbb{E}_{t-1}^{\mathbb{P}} [\exp(\varphi s_t)] = \mathbb{E}_{t-1}^{\mathbb{P}} \left[\exp \left(\varphi \frac{\psi_t' e_t}{\sqrt{\psi_t' \Sigma_{N_t} \psi_t}} \right) \right] = \mathbb{E}_{t-1}^{\mathbb{P}} \left[\mathbb{E}_{t-1}^{\mathbb{P}} \left[\exp \left(\varphi \frac{\psi_t' e_t}{\sqrt{\psi_t' \Sigma_{N_t} \psi_t}} \right) \middle| \psi_t \right] \right].$$

Under Assumption 4 where $e_t \sim N(0, \Sigma_{N_t})$ the MGF simplifies to

$$\mathbb{E}_{t-1}^{\mathbb{P}} \left[\exp \left(\varphi \frac{\psi_t' e_t}{\sqrt{\psi_t' \Sigma_{N_t} \psi_t}} \right) \middle| \psi_t \right] = \exp \left(\frac{1}{2} \frac{\varphi \psi_t'}{\sqrt{\psi_t' \Sigma_{N_t} \psi_t}} \Sigma_{N_t} \frac{\varphi \psi_t}{\sqrt{\psi_t' \Sigma_{N_t} \psi_t}} \right) = \exp \left(\frac{1}{2} \varphi^2 \right).$$

Therefore, the score, s_t , is i.i.d with a standard normal distribution under \mathbb{P} .

To derive the distribution under \mathbb{Q} , we first obtain,

$$\begin{aligned} & \mathbb{E}_t^{\mathbb{P}} [\exp(\varphi s_{t+1} + \phi_t R_{t+1} + \xi_t h_{t+2})] \\ &= \mathbb{E}_t^{\mathbb{P}} \left\{ \mathbb{E}_t^{\mathbb{P}} [\exp(\varphi s_{t+1} + \phi_t R_{t+1} + \xi_t h_{t+2}) | \phi_t R_{t+1}, \xi_t h_{t+2}, \psi_{t+1}] \right\} \\ &= \mathbb{E}_t^{\mathbb{P}} \left\{ \mathbb{E}_t^{\mathbb{P}} \left[\exp \left(\frac{1}{2} \varphi^2 + \phi_t R_{t+1} + \xi_t h_{t+2} \right) | \phi_t R_{t+1}, \xi_t h_{t+2}, \psi_{t+1} \right] \right\} \\ &= \exp \left(\frac{1}{2} \varphi^2 \right) \mathbb{E}_t^{\mathbb{P}} [\exp(\phi_t R_{t+1} + \xi_t h_{t+2})], \end{aligned}$$

where the last equality is a consequence of e_t being assumed to be independent of other variables. Next, we have

$$\mathbb{E}_t^{\mathbb{Q}} (\exp(\varphi s_{t+1})) = \frac{\mathbb{E}_t^{\mathbb{P}} [\exp(\varphi s_{t+1} + \phi_t R_{t+1} + \xi_t h_{t+2})]}{\mathbb{E}_t^{\mathbb{P}} [\exp(\phi_t R_{t+1} + \xi_t h_{t+2})]} = \exp \left(\frac{1}{2} \varphi^2 \right),$$

which shows that the score, s_t , is also i.i.d. and distributed as a standard normal under \mathbb{Q} .

A.5 Proof of Proposition 1

Let $\tilde{\boldsymbol{\eta}}_{t,M} = (\log \eta_{t+1}, \dots, \log \eta_{t+M})'$ and $\tilde{\boldsymbol{\eta}}_{t,M}^e = \mathbb{E}_t^{\mathbb{Q}}(\tilde{\boldsymbol{\eta}}_{t,M})$, where the latter embeds the expected path of $\log \eta_t$. The MGF for M -period cumulative returns $R_{t,M}$ can be expressed as

$$g_{t,M}(s) \equiv \mathbb{E}_t^{\mathbb{Q}}[\exp(sR_{t,M})] = \mathbb{E}_t^{\mathbb{Q}}\{\mathbb{E}_t^{\mathbb{Q}}[\exp(sR_{t,T}) \mid \tilde{\boldsymbol{\eta}}_{t,M}]\} = \mathbb{E}_t^{\mathbb{Q}}[f(\tilde{\boldsymbol{\eta}}_{t,M})],$$

where $f(\tilde{\boldsymbol{\eta}}_{t,M}) \equiv \mathbb{E}_t^{\mathbb{Q}}[\exp(sR_{t,T}) \mid \tilde{\boldsymbol{\eta}}_{t,M}]$. A second-order Taylor expansion of f around $\tilde{\boldsymbol{\eta}}_{t,M}^e$ gives us,

$$\begin{aligned} f(\tilde{\boldsymbol{\eta}}_{t,M}) &\approx f(\tilde{\boldsymbol{\eta}}_{t,M}^e) + \nabla'(\tilde{\boldsymbol{\eta}}_{t,M} - \tilde{\boldsymbol{\eta}}_{t,M}^e) + \frac{1}{2}(\tilde{\boldsymbol{\eta}}_{t,M} - \tilde{\boldsymbol{\eta}}_{t,M}^e)' \tilde{H}(\tilde{\boldsymbol{\eta}}_{t,M}^e, s)(\tilde{\boldsymbol{\eta}}_{t,M} - \tilde{\boldsymbol{\eta}}_{t,M}^e) \\ &= f(\tilde{\boldsymbol{\eta}}_{t,M}^e) + \nabla'(\tilde{\boldsymbol{\eta}}_{t,M} - \tilde{\boldsymbol{\eta}}_{t,M}^e) + \frac{1}{2} \text{tr} \left\{ \tilde{H}(\tilde{\boldsymbol{\eta}}_{t,M}^e, s) \boldsymbol{\varepsilon}_{t,M} \boldsymbol{\varepsilon}_{t,M}' \right\}, \end{aligned}$$

where

$$\tilde{H}(\tilde{\boldsymbol{\eta}}_{t,M}^e, s) = \left. \frac{\partial^2 f(\tilde{\boldsymbol{\eta}}_{t,M})}{\partial \tilde{\boldsymbol{\eta}}_{t,M} \partial \tilde{\boldsymbol{\eta}}_{t,M}'} \right|_{\tilde{\boldsymbol{\eta}}_{t,M} = \tilde{\boldsymbol{\eta}}_{t,M}^e},$$

is the Hessian, ∇ the Jacobian, and $\boldsymbol{\varepsilon}_{t,M} = \tilde{\boldsymbol{\eta}}_{t,M} - \tilde{\boldsymbol{\eta}}_{t,M}^e$. Since $\tilde{\boldsymbol{\eta}}_{t,M}^e \in \mathcal{G}_t$ and $f(\tilde{\boldsymbol{\eta}}_{t,M}^e) = g_{t,M}^*(s)$ we have

$$g_{t,M}(s) \approx g_{t,M}^*(s) + \frac{1}{2} \text{tr} \left\{ \tilde{H}(\tilde{\boldsymbol{\eta}}_{t,M}^e, s) \Sigma_M \right\}, \quad (\text{A.9})$$

where $\Sigma_M = \mathbb{E}_t^{\mathbb{Q}}[\boldsymbol{\varepsilon}_{t,M} \boldsymbol{\varepsilon}_{t,M}']$. From the AR(1) structure it follows that the m -th element of $\boldsymbol{\varepsilon}_{t,M}$ is given by, $[\boldsymbol{\varepsilon}_{t,M}]_m = \tilde{\eta}_{t+m} - \tilde{\eta}_{t+m}^e = \sum_{j=0}^{m-1} \theta^j \varepsilon_{t+m-j}$, $m = 1, \dots, M$, such that

$$\Sigma_M = \text{var}_t^{\mathbb{Q}} \left[\tilde{\boldsymbol{\eta}}_{t,M} - \tilde{\boldsymbol{\eta}}_{t,M}^e \right] = \text{var}_t^{\mathbb{Q}} (A_M \boldsymbol{\varepsilon}_{t,M}) = \sigma_e^2 A_M A_M',$$

where

$$[A_M]_{i,j} = \begin{cases} \theta^{i-j} & \text{for } i \geq j \\ 0 & \text{otherwise.} \end{cases}$$

The results above is for the AR(1) case. With an ARMA structure, $(1 - \theta(L)) \tilde{\eta}_t = (1 + \alpha(L)) \varepsilon_t$, we have

$$\tilde{\eta}_t = \frac{1 + \alpha(L)}{1 - \theta(L)} \varepsilon_t = \sum_{j=0}^{\infty} \psi_j \varepsilon_{t-j},$$

such that

$$[\boldsymbol{\varepsilon}_{t,M}]_m = \tilde{\eta}_{t+m} - \tilde{\eta}_{t+m}^e = \sum_{j=0}^{m-1} \psi_j \varepsilon_{t+m-j} = \sum_{j=1}^m \psi_{m-j} \varepsilon_{t+j}.$$

So in the more general ARMA case we have

$$[A_M]_{i,j} = \begin{cases} \psi_{i-j} & \text{for } i \geq j \\ 0 & \text{otherwise.} \end{cases}$$

A.5.1 The Hessian Matrix $\tilde{H}(\tilde{\boldsymbol{\eta}}_{t,M}^e, s)$

First, to simplify the notations, we suppress the dependence on T and s for most terms and write,

$$\begin{aligned} \omega_m &\equiv \omega_{T-m}^* = \omega\eta_{T-m}, \\ \alpha_m &\equiv \alpha_{T-m}^* = \alpha\eta_{T-m}\eta_{T-m-1}, \\ \beta_m &\equiv \beta_{T-m}^* = \beta\eta_{T-m}/\eta_{T-m-1}, \\ \gamma_m &\equiv \gamma_{T-m-1}^* = (\gamma + \lambda - \frac{1}{2})/\eta_{T-m-1} + \frac{1}{2}, \end{aligned}$$

$A(M) \equiv A_T(s, M)$, and $B(M) \equiv B_T(s, M)$. For derivatives of a variable Y we write

$$Y^{(i)} \equiv \frac{\partial Y}{\partial \tilde{\eta}_{t+i}} \quad \text{and} \quad Y^{(i,j)} \equiv \frac{\partial^2 Y}{\partial \tilde{\eta}_{t+i} \partial \tilde{\eta}_{t+j}}.$$

From Theorem 3 we have $f(\tilde{\boldsymbol{\eta}}_{t,M}) = \exp\{A(M) + B(M)h_{t+1}^*\}$ with first and second derivatives given by

$$f^{(i)} = f(\tilde{\boldsymbol{\eta}}_{t,M})[A^{(i)}(M) + B^{(i)}(M)h_{t+1}^*],$$

and

$$\begin{aligned} f^{(i,j)} &= f(\tilde{\boldsymbol{\eta}}_{0,M})[A^{(i)}(M) + B^{(i)}(M)h_{t+1}^*][A^{(j)}(M) + B^{(j)}(M)h_{t+1}^*] \\ &\quad + f(\tilde{\boldsymbol{\eta}}_{0,M})[A^{(i,j)}(M) + B^{(i,j)}(M)h_{t+1}^*], \end{aligned}$$

respectively. From the expression for $A(M)$ and $B(M)$ in Theorem 3, we find (for the first derivatives)

$$A^{(i)}(m+1) = A^{(i)}(m) + \omega_m^{(i)} B(m) + \omega_m B^{(i)}(m) + \frac{\alpha_m^{(i)} B(m) + \alpha_m B^{(i)}(m)}{1 - 2\alpha_m B(m)}, \quad (\text{A.10})$$

$$\begin{aligned} B^{(i)}(m+1) &= (s - \gamma_m)\gamma_m^{(i)} + \beta_m B^{(i)}(m) + \beta_m^{(i)} B(m) \\ &\quad + (s - \gamma_m)^2 \frac{\alpha_m^{(i)} B(m) + \alpha_m B^{(i)}(m)}{[1 - 2\alpha_m B(m)]^2} + (\gamma_m - s) \frac{\gamma_m^{(i)}}{[1 - 2\alpha_m B(m)]}, \end{aligned} \quad (\text{A.11})$$

with $A^{(i)}(1) = B^{(i)}(1) = 0$. Similarly, for the second derivatives we find

$$\begin{aligned}
A^{(i,j)}(m+1) &= A^{(i,j)}(m) + \omega_m^{(i,j)}B(m) + \omega_m^{(i)}B^{(j)}(m) + B^{(i)}(m)\omega_m^{(j)} + \omega_m B^{(i,j)}(m) \\
&\quad + \frac{1}{[1-2\alpha_m B(m)]} \left(\alpha_m^{(i,j)}B(m) + \alpha_m^{(i)}B^{(j)}(m) + B^{(i)}(m)\alpha_m^{(j)} + \alpha_m B^{(i,j)}(m) \right) \\
&\quad + \frac{2}{[1-2\alpha_m B(m)]^2} \left(\alpha_m^{(i)}B(m) + \alpha_m B^{(i)}(m) \right) \left(\alpha_m^{(j)}B(m) + \alpha_m B^{(j)}(m) \right), \\
B^{(i,j)}(m+1) &= \beta_m^{(i,j)}B(m) + \beta_m^{(i)}B^{(j)}(m) + B^{(i)}(m)\beta_m^{(j)} + \beta_m B^{(i,j)}(m) \\
&\quad + \frac{2\alpha_m B(m)}{[1-2\alpha_m B(m)]} \left[\gamma_m^{(i)}\gamma_m^{(j)} + (\gamma_m - s)\gamma_m^{(i,j)} \right] \\
&\quad + \frac{2(\gamma_m - s)}{[1-2\alpha_m B(m)]^2} \left[\left(\alpha_m^{(i)}B(m) + \alpha_m B^{(i)}(m) \right) \gamma_m^{(j)} + \gamma_m^{(i)} \left(\alpha_m^{(j)}B(m) + \alpha_m B^{(j)}(m) \right) \right] \\
&\quad + \frac{(s-\gamma_m)^2}{[1-2\alpha_m B(m)]^2} \left(\alpha_m^{(i,j)}B(m) + \alpha_m^{(i)}B^{(j)}(m) + B^{(i)}(m)\alpha_m^{(j)} + \alpha_m B^{(i,j)}(m) \right) \\
&\quad + \frac{4(s-\gamma_m)^2}{[1-2\alpha_m B(m)]^3} \left(\alpha_m^{(i)}B(m) + \alpha_m B^{(i)}(m) \right) \left(\alpha_m^{(j)}B(m) + \alpha_m B^{(j)}(m) \right),
\end{aligned}$$

with $A^{(i,j)}(1) = B^{(i,j)}(1) = 0$ and

$$\begin{aligned}
\omega_m^{(i)} &= \begin{cases} \omega_m & \text{for } i = m, \\ 0 & \text{otherwise,} \end{cases} \quad \alpha_m^{(i)} = \begin{cases} \alpha_m & \text{for } i = m, m+1, \\ 0 & \text{otherwise,} \end{cases}, \\
\beta_m^{(i)} &= \begin{cases} \beta_m & \text{for } i = m \\ -\beta_m & \text{for } i = m+1, \\ 0 & \text{otherwise,} \end{cases} \quad \gamma_m^{(i)} = \begin{cases} \gamma_m - \frac{1}{2} & \text{for } i = m+1, \\ 0 & \text{otherwise,} \end{cases}, \\
\omega_m^{(i,j)} &= \begin{cases} \omega_m & \text{for } i = j = m, \\ 0 & \text{otherwise,} \end{cases}, \quad \alpha_m^{(i,j)} = \begin{cases} \alpha_m & \text{for } i, j = m, m+1, \\ 0 & \text{otherwise,} \end{cases}, \\
\beta_m^{(i,j)} &= \begin{cases} \beta_m & \text{for } i = j \in \{m, m+1\} \\ -\beta_m & \text{for } i \neq j \in \{m, m+1\}, \\ 0 & \text{otherwise,} \end{cases} \quad \gamma_m^{(i,j)} = \begin{cases} \gamma_m - \frac{1}{2} & \text{for } i = j = m+1 \\ 0 & \text{otherwise.} \end{cases}
\end{aligned}$$

Finally, the scaled Hessian matrix presented in Theorem 1 is defined by $H(\tilde{\boldsymbol{\eta}}_{t,M}^e, s) = \frac{1}{g_{t,M}^*(s)} \tilde{H}(\tilde{\boldsymbol{\eta}}_{t,M}^e, s)$. We adopt his formulation because it simplifies the expression.

A.6 The Scores for Derivatives

A.6.1 Score for VIX

The case, $X_t = \log \text{VIX}_t$, where $N_t = 1$, is the simplest case to drive the score for. The log-likelihood function for $\ell(\text{VIX}_t | \mathcal{G}_t)$ is here given by

$$\ell(\text{VIX}_t | \mathcal{G}_t) = -\frac{1}{2\sigma_e^2} (\log \text{VIX}_t - \log \text{VIX}_t^m)^2,$$

and its first derivative is,

$$\nabla_t = \frac{1}{\sigma_e^2} (\log \text{VIX}_t - \log \text{VIX}_t^m) \left(\frac{\partial \log \text{VIX}_t^m}{\partial \log \eta_t} \right).$$

The conditional variance of ∇_t is

$$\mathbb{E}^{\mathbb{P}}[\nabla_t^2 | \mathcal{G}_t] = \frac{1}{\sigma_e^2} \left(\frac{\partial \log \text{VIX}_t^m}{\partial \log \eta_t} \right)^2,$$

and it follows that

$$s_t = \frac{1}{\sigma_e} (\log \text{VIX}_t - \log \text{VIX}_t^m) \text{sign} \left(\frac{\partial \log \text{VIX}_t^m}{\partial \log \eta_t} \right).$$

For the last term, we recall the expression, $\text{VIX}_t^m = \sqrt{a_1(\eta_t, M, \sigma^2) + a_2(\eta_t, M, \sigma^2)h_{t+1}^*}$, which leads to the the expression

$$\frac{\partial \log \text{VIX}_t^m}{\partial \log \eta_t} = \frac{1}{2(\text{VIX}_t^m)^2} \left[\frac{\partial a_{1,t}}{\partial \log \eta_t} + \left(\frac{\partial a_{2,t}}{\partial \log \eta_t} + a_{2,t} \right) h_{t+1}^* \right]$$

where the terms

$$\begin{aligned} \frac{\partial a_{1,t}}{\partial \log \eta_t} &= \frac{A^2}{M} \sum_{k=2}^M \sum_{i=2}^k \tilde{\beta}^{k-i} \left[\omega \Lambda_1(k) \theta^{k-1} \eta_t^{\theta^{k-1}} + \alpha \Lambda_2(k, i) (\theta^{k-1} + \theta^{i-2}) \eta_t^{(\theta^{k-1} + \theta^{i-2})} \right], \\ \frac{\partial a_{2,t}}{\partial \log \eta_t} + a_{2,t} &= \frac{A^2}{M} \sum_{k=1}^M \tilde{\beta}^{k-1} \Lambda_1(k) \theta^{k-1} \eta_t^{(\theta^{k-1}-1)}, \end{aligned}$$

are positive. The term, $\text{sign} \left(\frac{\partial \log \text{VIX}_t^m}{\partial \log \eta_t} \right)$, is therefore redundant and we arrived at the simple expression,

$$s_t = \frac{1}{\sigma_e} (\log \text{VIX}_t - \log \text{VIX}_t^m).$$

By Assumption 4 it follows that s_t is i.i.d a standard normally distributed.

A.6.2 Score for Option Prices

When the model is estimated with option prices, the elements of $X_t \in \mathbb{R}^{N_t}$ are given by

$$\log(\text{IV}_{bs}(C_t, S_t, M, K, r)),$$

for the N_t options selected at time t . The logarithm of Black-Scholes implied volatility makes this variable comparable to $\log \text{VIX}_t$, which is used when the model is estimated with VIX data.

Let X_t^m denote the logarithm of model-based implied volatility for a particular option.

We seek an expression for

$$\frac{\partial X_t^m}{\partial \log \eta_t} = \frac{\partial \log(\text{IV}_{bs}^m)}{\partial \text{IV}_{bs}^m} \frac{\partial \text{IV}_{bs}^m}{\partial C_t^m} \frac{\partial C_t^m}{\partial \log \eta_t} = \frac{\text{Vega}_{bs}^m}{\text{IV}_{bs}^m} \frac{\partial C_t^m}{\partial \log \eta_t},$$

where

$$\text{Vega}_{bs} = \frac{1}{\sqrt{2\pi}} \exp\left(-\frac{1}{2}d_t^2\right) S_t \sqrt{M},$$

is the Black-Scholes implied Vega and

$$d_t = \frac{1}{\text{IV}_{bs} \sqrt{M}} \left[\log\left(\frac{S_t}{K}\right) + \left(r + \frac{\text{IV}_{bs}^2}{2}\right) M \right].$$

For $\partial \hat{C}^m / \partial \log \eta_t$, we find

$$\frac{\partial \hat{C}^m(S_t, M, K, r; h_{t+1}^*)}{\partial \log \eta_t} = S_t \frac{\partial P_1(t)}{\partial \log \eta_t} - K \exp(-rM) \frac{\partial P_2(t)}{\partial \log \eta_t},$$

where

$$\begin{aligned} \frac{\partial P_1(t)}{\partial \log \eta_t} &= \frac{\exp(-rM)}{\pi} \int_0^\infty \text{Re} \left[\frac{K^{-i\varphi}}{i\varphi S_t} \frac{\partial \hat{g}_{t,M}(i\varphi + 1)}{\partial \log \eta_t} \right] d\varphi, \\ \frac{\partial P_2(t)}{\partial \log \eta_t} &= \frac{1}{\pi} \int_0^\infty \text{Re} \left[\frac{K^{-i\varphi}}{i\varphi} \frac{\partial \hat{g}_{t,M}(i\varphi)}{\partial \log \eta_t} \right] d\varphi, \end{aligned}$$

with

$$\hat{g}_{t,M}(s) = g_{t,M}^*(s) \left[1 + \frac{1}{2} \text{tr}(H_{t,M}(s) \Sigma_M) \right].$$

Using the simplified notations in Section A.5.1, we have

$$\frac{\partial \hat{g}_{t,M}(s)}{\partial \log \eta_t} = \hat{g}_{t,M}(s) \left(A^{(0)}(M) + \left(B^{(0)}(M) + B(M) \right) h_{t+1}^* \right) + \frac{1}{2} g_{t,M}^*(s) \text{tr} \left(\dot{H}_{t,M}(s) \Sigma_M \right), \quad (\text{A.12})$$

which is the expression we use to price options with the second-order approximation. Pricing options with first-order approximation, amounts to dropping the last term in (A.12). With a first-order approximation, we simply need to compute $A^{(0)}(m)$ and $B^{(0)}(m)$, that are given recursively from (A.10) and (A.11), with initial condition $\dot{A}(1) = \dot{B}(1) = 0$, and use

$$\begin{aligned} \omega_m &= \omega \Psi_t(M - m + 1), \\ \alpha_m &= \alpha \Psi_t(M - m + 1) \Psi_t(M - m), \\ \beta_m &= \beta \Psi_t(M - m + 1) / \Psi_t(M - m), \\ \gamma_m &= (\gamma + \lambda - \frac{1}{2}) / \Psi_t(M - m) + \frac{1}{2}, \end{aligned}$$

where $\Psi_t(k)$ is defined as

$$\Psi_t(k) = \exp \{ \mathbb{E}_t(\log \eta_{t+k-1}) \} = \exp \left\{ (1 - \theta^{k-1}) \zeta + \theta^{k-1} \log \eta_t \right\}.$$

The corresponding first derivatives (with respect to $\log \eta_t$) are given by

$$\begin{aligned} \dot{\omega}_m &= \omega_m \theta^{M-m}, \\ \dot{\alpha}_m &= \alpha_m \left(\theta^{M-m} + \theta^{M-m-1} \right), \\ \dot{\beta}_m &= \beta_m \left(\theta^{M-m} - \theta^{M-m-1} \right), \\ \dot{\gamma}_m &= \left(\frac{1}{2} - \gamma_m \right) \theta^{M-m-1}. \end{aligned}$$

For the second-order approximation in (A.12), we need to evaluate $\dot{H}_{t,M}(s) = \partial H_{t,M}(s) / \partial \log \eta_t$, for which we have

$$\begin{aligned} \dot{H}_{i,j} &= \left(A^{(i,0)}(M) + B^{(i,0)}(M) h_{t+1}^* \right) \left(A^{(j)}(M) + B^{(j)}(M) h_{t+1}^* \right) \\ &\quad + \left(A^{(i)}(M) + B^{(i)}(M) h_{t+1}^* \right) \left(\dot{A}^{(j)}(M) + \dot{B}^{(j)}(M) h_{t+1}^* \right) \\ &\quad + \left(A^{(i,j,0)}(M) + B^{(i,j,0)}(M) h_{t+1}^* \right). \end{aligned}$$

The expressions for the third derivatives, $A^{(i,j,0)}(m) = \partial A^{(i,j,0)}(m) / \partial \log \eta_t$ and $B^{(i,j,0)}(m) = \partial B^{(i,j,0)}(m) / \partial \log \eta_t$ are relatively cumbersome, and are omitted to conserve space.

We now have all the terms needed for the analytical formula for $\partial C^m / \partial \log \eta_t$. In practice, however, it may be more convenient to compute this derivative with numerical methods, i.e.

$$\frac{\partial C_t^m}{\partial \log \eta_t} \approx \frac{1}{\Delta} [C_t^m(\log \eta_t + \Delta) - C_t^m(\log \eta_t)]$$

for a very small value of Δ , because this simplifies the calculation of score with respect to option prices, and is very fast.

A.7 Computing Moments by the Characteristic Function

The k -th moment of cumulative returns can be expressed as

$$\mathbb{E} \left(R^k \right) = \int_{-\infty}^{+\infty} R^k f(R) dR = \underbrace{\int_{-\infty}^0 R^k f(R) dR}_{(*)} + \underbrace{\int_0^{+\infty} R^k f(R) dR}_{(**)},$$

where $f(R)$ is the conditional density of cumulated returns under \mathbb{Q} . By the Fourier inverse transform, $f(R)$ can be expressed as

$$f(R) = \frac{1}{\pi} \int_0^{\infty} \text{Re} \left[e^{-uR} \phi(u) \right] du_I, \quad \phi(u) \equiv \mathbb{E} \left[e^{uR} \right],$$

where $u = u_R + iu_I \in \mathbb{C}$, with $u_R = \text{Re}[u]$ being the real part of u , and $\phi(u)$ is the characteristic function of cumulated returns.

Then after changing the order of integration by Fubini's theorem, we find

$$\begin{aligned} (*) &= \frac{1}{\pi} \int_0^\infty \text{Re} \left[\left(\int_{-\infty}^0 R^k e^{-uR} dR \right) \phi(u) \right] du_I, \\ (**) &= \frac{1}{\pi} \int_0^\infty \text{Re} \left[\left(\int_0^{+\infty} R^k e^{-vR} dR \right) \phi(v) \right] dv_I. \end{aligned}$$

We have here used the following Laplace transformations for R^k :

$$\begin{aligned} \int_{-\infty}^0 R^k e^{-uR} dR &= -\frac{k!}{u^{k+1}}, \quad u_R < 0, \\ \int_0^{+\infty} R^k e^{-vR} dR &= \frac{k!}{v^{k+1}}, \quad v_R > 0. \end{aligned}$$

Thus, it follows that

$$\begin{aligned} (*) &= \frac{1}{\pi} \int_0^\infty \text{Re} \left[-\frac{k}{u^{k+1}} \phi(u) \right] du_I, \\ (**) &= \frac{1}{\pi} \int_0^\infty \text{Re} \left[\frac{k}{v^{k+1}} \phi(v) \right] dv_I. \end{aligned}$$

A.8 Computation of Option Prices by Numerical Integrations

Our expression for option prices in Theorem 3 requires the evaluation of integrals of the type, $\int_0^\infty f(x)dx$, for the computation of $P_1(t)$ and $P_2(t)$. For this, we use the Gauss-Laguerre quadrature method, which is an extension of the Gaussian quadrature method for approximating the value of integrals of the following kind:

$$\int_0^\infty e^{-x} g(x) dx \approx \sum_{i=1}^L w(x_i) g(x_i).$$

The Gauss-Laguerre quadrature method is also based the abscissae x_1, \dots, x_L and their associated weights $w(x_i)$ with $i = 1, \dots, L$, leading to the following numerical approximation,

$$\int_0^\infty f(x) dx = \int_0^\infty e^{-x} [e^x f(x)] dx \approx \sum_{i=1}^L w(x_i) e^{x_i} f(x_i).$$

In our implementation we use $L = 32$.

B Supplementary Empirical Results

B.1 Alternative RMSE Measure

An alternative metric for evaluation the derivative pricing is to compute the RMSE in volatility levels. For the VIX this is defined by

$$\text{RMSE}_{\text{VIX}} = \sqrt{\frac{1}{T} \sum_{t=1}^T [\text{VIX}_t^m - \text{VIX}_t]^2},$$

and for option prices it is defined by

$$\text{RMSE}_{\text{IV}} = \sqrt{\frac{1}{\sum_{t=1}^T N_t} \sum_{t=1}^T \sum_{i=1}^{N_t} [\text{IV}_{t,i}^m - \text{IV}_{t,i}]^2} \times 100.$$

The results for the RMSE in volatility levels are reported in Tables B.1 and B.2, where the former is analogous to Table 3 and the latter is analogous to the out-of-sample results in Table 4. The results are qualitatively very similar to the RMSE for logarithmically transformed volatilities in Tables 3 and 4.

B.2 A Variance Risk Ratio based on Model-Free Realized Variances

As a robustness check we compute an alternative monthly measure of the variance risk ratio, $\tilde{\eta} = \frac{\text{VIX}^2}{\sigma_{\mathbb{P}}^2}$, where $\sigma_{\mathbb{P}}^2$ is an empirical measure of the expected variance under \mathbb{P} , deduced from monthly realized variances. So, $\sigma_{\mathbb{P}}^2$ does not rely on the Heston-Nandi GARCH model. The monthly realized variance for the S&P 500 index is computed as the sum of squared 5-minute intraday returns during the hours from 9:30 AM to 4:00 PM plus the sum of squared overnight returns. This quantity is multiplied by 12×100^2 to bring it to the same scale as the VIX^2 (squared annualized percentage). Finally, $\sigma_{\mathbb{P}}^2$ is defined to be the one-month ahead prediction of the monthly realized variance using a AR(1) model.

This time-series of this empirical variance risk ratios is presented in Figure B.1, and it is very similar to the model-based time-series presented in Figure 5.

Figure B.2 contains scatterplots of volatility prediction errors under \mathbb{P} and the level of $\log \eta$. The former is defined as the difference between the ex-post model-implied variance and the ex-ante model-based one-month ahead volatility prediction. The scatterplots indicate some positive correlation, but we do not find that a large proportion of overpredictions of volatility occurs when $\log \eta_t$ is relatively small, nor that a large proportion of underpredictions of volatility occurs when $\log \eta_t$ is large.

Table B.1: VIX and Option Pricing Performance (RMSE)

Model	CHNG [VIX]	CHNG [Opt]	SHNG [VIX]	SHNG [Opt]
<i>A: RMSE for VIX Pricing</i>				
Full Sample	4.117	4.143	1.024	1.795
<i>B: RMSE for Option Pricing</i>				
Full Sample	4.277	4.151	2.327	1.746
<i>Partitioned by moneyness</i>				
Delta<0.3	4.500	4.149	3.108	1.947
0.3≤Delta<0.4	4.069	3.985	2.830	1.859
0.4≤Delta<0.5	3.743	3.862	2.415	1.639
0.5≤Delta<0.6	3.798	3.999	2.033	1.444
0.6≤Delta<0.7	4.017	4.062	1.876	1.455
0.7≤Delta	4.771	4.417	2.098	1.949
<i>Partitioned by maturity</i>				
DTM<30	4.649	4.110	2.385	2.252
30≤DTM<60	4.235	4.058	2.061	1.475
60≤DTM<90	4.065	4.086	2.156	1.311
90≤DTM<120	4.059	4.234	2.492	1.598
120≤DTM<150	4.073	4.212	2.623	1.781
150≤DTM	4.192	4.537	2.757	1.819
<i>Partitioned by the level of VIX</i>				
VIX<15	3.726	3.727	1.821	1.155
15≤VIX<20	2.980	3.252	2.051	1.438
20≤VIX<25	3.711	3.808	2.265	1.718
25≤VIX<30	4.525	4.266	2.703	2.126
30≤VIX<35	5.460	5.227	3.071	2.444
35≤VIX	10.68	9.164	4.727	4.089

Note: This table reports the in-sample VIX and option pricing performance for each model in Table 2. We evaluate the model's option pricing ability through the root of mean square errors of implied volatility ($RMSE_{IV}$). We summarize the results by option moneyness, maturity and market VIX level. Moneyness is measured by Delta computed from the Black-Scholes model. DTM denotes the number of calendar days to maturity. The numbers in bold indicate the minimum value within each row in each time period.

Table B.2: Out-of-sample VIX and Option Pricing (RMSE)

Model	CHNG [VIX]	CHNG [Opt]	SHNG [VIX]	SHNG [Opt]
<i>A: RMSE for VIX Pricing</i>				
Full Sample	5.083	4.660	1.278	2.067
<i>B: RMSE for Option Pricing</i>				
Full Sample	4.710	4.043	2.724	1.932
<i>Partitioned by moneyness</i>				
Delta<0.3	4.973	4.068	3.839	2.108
0.3≤Delta<0.4	4.622	3.910	3.467	2.018
0.4≤Delta<0.5	4.255	3.709	2.849	1.701
0.5≤Delta<0.6	4.339	3.907	2.281	1.508
0.6≤Delta<0.7	4.696	4.108	2.021	1.635
0.7≤Delta	4.934	4.213	2.202	2.195
<i>Partitioned by maturity</i>				
DTM<30	5.276	4.243	2.858	2.301
30≤DTM<60	4.692	3.968	2.526	1.591
60≤DTM<90	4.217	3.794	2.547	1.524
90≤DTM<120	4.317	4.013	2.758	1.818
120≤DTM<150	4.133	3.870	2.941	2.157
150≤DTM	4.263	4.182	2.965	2.117
<i>Partitioned by the level of VIX</i>				
VIX<15	4.062	3.121	2.003	1.257
15≤VIX<20	3.081	3.060	2.403	1.531
20≤VIX<25	3.026	3.537	2.615	1.714
25≤VIX<30	4.073	3.902	3.169	2.287
30≤VIX<35	5.352	4.856	3.688	2.719
35≤VIX	12.05	9.423	5.199	4.376

Note: This table report the out-of-sample option pricing performance for each model. We conduct our out-of-sample performance evaluation by splitting our original dataset into two subsamples: the in-sample data consists of the years before 2008 and the out-of-sample consists of the years 2008-2021, which spans a 14-year period. The estimation for each model is done only once for the in-sample data, and then price the out-of-sample data by the estimated parameters. Therefore, the in-sample data is 1990-2007. We evaluate the model's option pricing ability through the root of mean square errors of implied volatility (IVRMSE). We summarize the results by option moneyness, maturity and market VIX level. Moneyness is measured by Delta computed from the Black-Scholes model. DTM denotes the number of calendar days to maturity. The numbers in shaded region indicate the minimum value within each row in each time period..

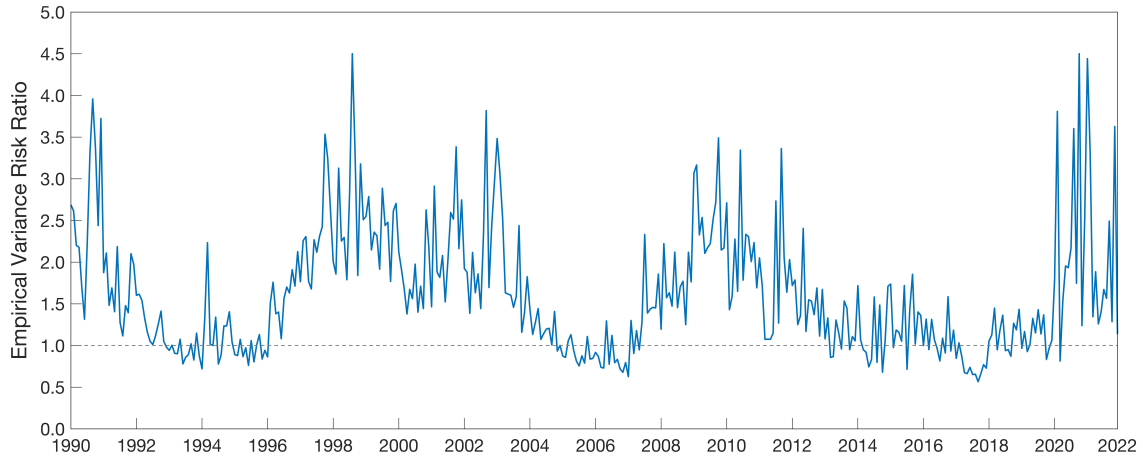


Figure B.1: An empirical monthly variance risk ratio, defined as the ratio of VIX_t^2 and the predicted value of the monthly realized variance using an AR(1) model.

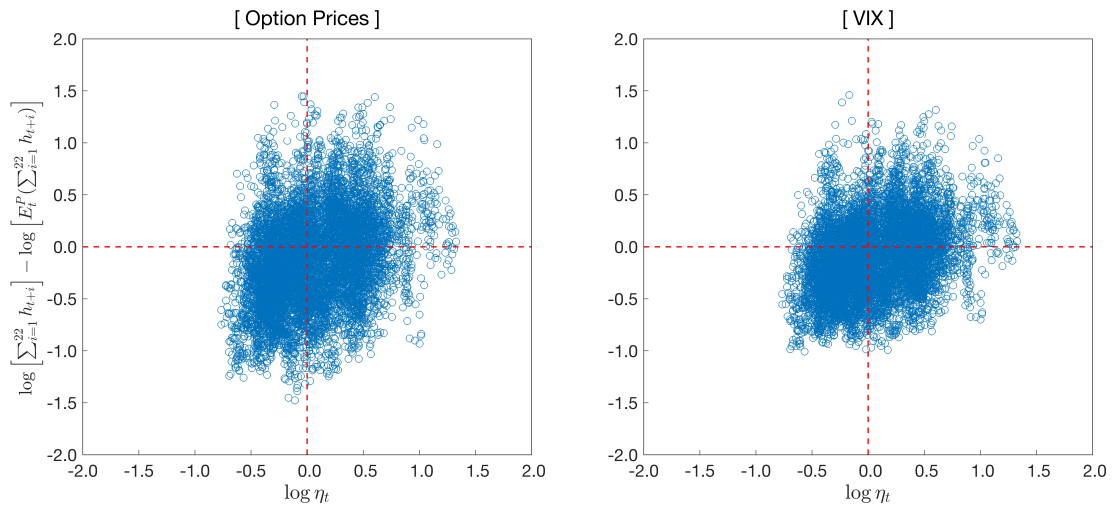


Figure B.2: The relations between SHNG model-implied logarithm of variance risk ratio and one-month ahead volatility prediction errors.